JOURNAL OF GEOPHYSICAL RESEARCH, VOL. 98, NO. B4, PAGES 6805–6827, APRIL 10, 1993

Rise and Tilt of Metamorphic Rocks in the Lower Plate of a Detachment Fault in the Funeral Mountains, Death Valley, California

THOMAS D. HOISCH

U.S. Geological Survey and Department of Geology, Northern Arizona University, Flagstaff, Arizona

CAROL SIMPSON

Department of Earth and Planetary Sciences, Johns Hopkins University, Baltimore, Maryland

The Funeral Mountains in eastern California preserve a record of Early Cretaceous (?) metamorphism followed by ductile deformation, uplift, and low-angle normal (detachment) faulting. $^{40}Ar/^{39}Ar$ age spectra indicate that cooling and uplift of the lower plate began in Cretaceous time. Uplift was accommodated by normal-sense movement along a wide northwest dipping shear zone. Mylonitic fabrics, some of which have been dated as Late Cretaceous, deformed older high-temperature metamorphic textures. Analyses of shear bands, mica fish, σ and δ porphyroclasts, grain shape fabrics, and folds indicate that the upper surfaces moved toward 299° ± 12 (top to the northwest) relative to lower surfaces. Uplift continued until the near present, the youngest phase being accommodated by top-to-the-northwest movement along the detachment fault, which formed subparallel to lower-plate mylonitic fabrics. Fission track apatite data indicate that exposure of the lower plate to the surface occurred sometime after 6 Ma. Reconstruction along the movement vector places the Grapevine Mountains over the Funeral Mountains, having been displaced at least 40 km. Isograds and thermobarometry in pelitic schist from the lower plate indicate increasing pressures and temperatures of equilibration toward the northwest. The maximum temperature and pressure was determined on a sample from Monarch Canyon using thermobarometry, 700°C at a depth of 32 km. At Chloride Cliff, 5 km southeast of Monarch Canyon, 4 samples yielded 575°–600°C at depths of 19–27 km. At Indian Pass, 17 km southeast of Monarch Canyon, a temperature of 490°C was determined. In the southern Funeral Mountains, about 50 km southeast of Monarch Canyon, conodont color alteration indexes indicate temperatures of 325°–425°C. These data indicate that the lower plate is presently tilted strongly to the southeast from the orientation it maintained at the peak of metamorphism. Thermochronologic data (K-Ar on muscovite, biotite, and hornblende, $^{40}Ar/^{39}Ar$ on hornblende, and fission track on apatite, titanite, and zircon) indicate that both tilting and the transition from ductile to brittle styles of quartz deformation are confined to the interval 21–6 Ma; during the latter part of this interval (11–6 Ma), rapid uplift and movement along the detachment fault are documented. The findings support current theories of detachment fault evolution in which a dipping fault surface undergoes rotation to a subhorizontal orientation while the lower plate undergoes a comparable tilt.

INTRODUCTION

Several models have been recently proposed for the evolution of detachment (low-angle normal) faults [*Buck*, 1988; *Hamilton*, 1988*a*, *b*; *Wernicke and Axen*, 1988; *Spencer and Reynolds*, 1991]. These models, although different in their details, all share the concept that detachment faults undergo rotation from a gentle or moderate dip to subhorizontal, while the lower plate undergoes a comparable tilt. This aspect of the models may be investigated by studying rocks in the lower plate, integrating pressure-temperature-time (P-T-t) paths, determined from thermochronologic and thermobarometric data, with kinematic data and mapping. The northern Funeral Mountains, which form part of the northeastern flank of Death Valley in eastern California (Figure 1), provide an ideal setting in which to investigate crustal extension. In this area, a detachment fault of Tertiary age is exposed. Lower-plate rocks preserve an Early Cretaceous (?) metamorphism ranging up to upper amphibolite faces in grade and are well suited for thermobarometric and thermochronologic study. Upper-plate rocks are much lower in grade (low to subgreenschist facies).

Paper number 92JB02411.
0148-0227/93/92JB-02411$05.00

Mylonitic fabrics and ductile folds which developed during cooling and uplift in the lower plate provide numerous indications of shear sense. These characteristics make it possible to evaluate whether the lower plate underwent tilting contemporaneous with fault movement.

This study attempts to integrate data from this and previous studies into a coherent interpretation of the lower plate's evolution. Added are new thermobarometric data from unsheared metamorphic rocks, kinematic analysis of mylonitic fabrics and ductile folding, and new geochronologic data (fission track, K-Ar, and $^{40}Ar/^{39}Ar$), to previous petrologic [*Giaramita*, 1984; *Hodges and Walker*, 1990; *Labotka*, 1980; *Labotka and Albee*, 1988], geochronologic [*Applegate et al.*, 1992; *DeWitt et al.*, 1988; *Holm and Dokka*, 1991], and mapping studies [*Applegate et al.*, 1992; *McAllister*, 1971; *Troxel and Wright*, 1989]. One hundred twenty samples distributed among seventy collection sites were taken from four areas within the northern and central Funeral Mountains. Only a fraction of these samples produced viable thermobarometric, mineral assemblage, or kinematic data. Twenty-three of the samples were oriented for thin-section analysis of shear sense from microstructural rotational strain indicators. Measurements of mesoscale asymmetric porphyroclasts and ductile folds provided further indications of shear sense. The grain size in quartz mylonites was used to

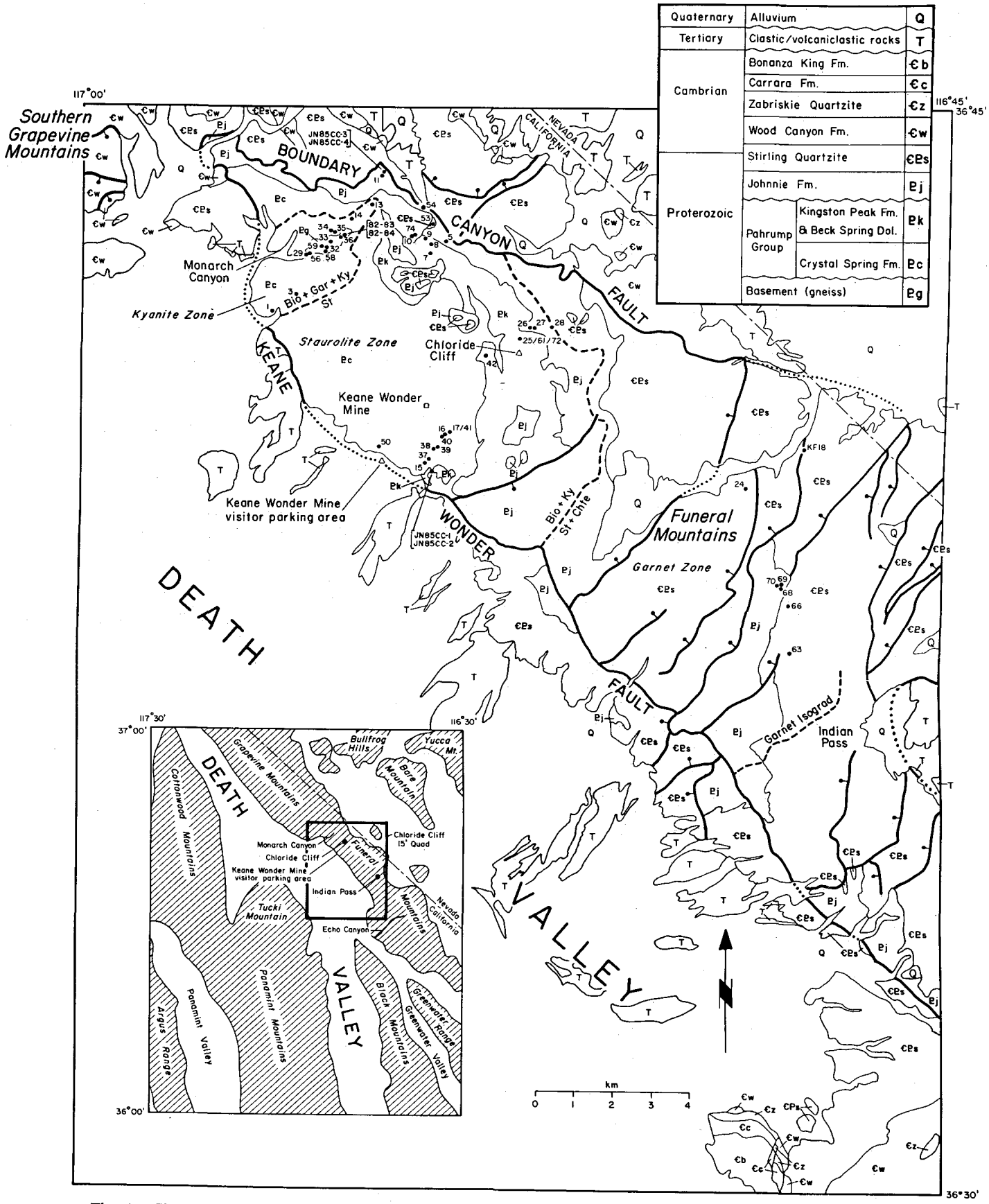

Fig. 1. Simplified geologic map of the Chloride Cliff 15′ quadrangle showing sample locations, three isograds, major faults, rocks units, and names of locations mentioned in the text. Geology based on mapping by *Troxel and Wright* [1989] and isograds based on *Labotka and Albee*'s [1988] study with minor modification. Two isograds are labeled with mineral reactions (see Table 1*a* for mineral abbreviations). Numbers indicate sample stations, with "CC-" omitted for clarity. "KF18" is a sample station provided by K. F. Fox, Jr. Samples CC-32a and CC-32b, shown in Figure 2 and 7*c*, respectively, were collected approximately 20 m apart. Other sample stations represent single outcrops. Some sample stations represent the same site, having been revisited and recollected (CC-17/41 and CC-25/61/72).

place limits on the temperatures associated with the lower-temperature deformation.

GEOLOGY OF THE NORTHERN FUNERAL MOUNTAINS

Rocks in the Funeral Mountains belong mainly to a thick sedimentary succession deposited in Late Proterozoic through Paleozoic time. The basement to this succession is exposed in Monarch Canyon (Figure 1) and consists of a complex of igneous and metamorphic rocks that has been dated using U-Pb methods at 1.7 Ga (R. E. Zartman as reported by *Wright and Troxel* [1993]). The oldest units in the succession belong to the Late Proterozoic Pahrump Group, which consists of the Crystal Spring Formation, Beck Spring Dolomite, and Kingston Peak Formation (oldest to youngest). This is unconformably overlain by the Late Proterozoic Johnnie Formation, Late Proterozoic to Early Cambrian Stirling Quartzite and Cambrian Wood Canyon Formation [*Troxel and Wright*, 1989]. *Applegate et al.* [1992] recently included part of the Late Proterozoic Noonday Dolomite, a thin unit (250–450 m thick [*Hunt and Mabey*, 1966]) which conformably underlies the Johnnie Formation, in the northern Funeral Mountains section. The thickness from the base of the Pahrump Group to the top of the Stirling Quartzite, excluding the Noonday Dolomite (following *Troxel and Wright* [1989]), is about 6 km [*Hunt and Mabey*, 1966; *Stewart*, 1970]. The Wood Canyon Formation forms the base of a 6 to 7-km-thick succession of Paleozoic strata [*Hunt and Mabey*, 1966]; however, components younger than Cambrian are not present in the northern Funeral Mountains. Lower-plate rocks comprise strata older than the middle part of the Stirling Quartzite, and upper plate rocks comprise younger strata. Along the flanks of the range in the upper plate, a succession of nonmetamorphosed Tertiary clastic, volcanic, and volcaniclastic units unconformably overlie Wood Canyon and Stirling Formations [*Troxel and Wright*, 1989].

The structure of the northern Funeral Mountains is elucidated in mapping by *Troxel and Wright* [1989] at 1:48,000 scale (Figure 1 provides a generalization). The most prominent structural feature is the detachment fault, which wraps around the northern end of the range and trends subparallel to the northeastern and southwestern flanks. The part of the fault exposed along the northeastern flank is known as the Boundary Canyon fault (Figure 1), and the part exposed along the southwestern flank is known as the Keane Wonder fault (Figure 1). *Reynolds* [1976], *Giaramita* [1984], and *Troxel and Wright* [1989] mapped the continuity between the two faults around the northwestern corner of the Funeral Mountains, and *Hamilton* [1988*a*, *b*] proposed that the two faults represent a single domiform surface. In the northern Funeral Mountains, the surface is antiformal in shape with the axis trending and gently plunging to the northwest. The lower plate is a largely contiguous structural block, broken only by Tertiary normal faults and by a southeast vergent thrust fault in the southern part of the range (referred to as the Schwaub Peak thrust by *Troxel and Wright* [1989] and *Wernicke et al.* [1988]). A klippe of upper-plate Tertiary rocks is present in the central Funeral Mountains about 5 km southeast of Indian Pass (truncated along the eastern margin of Figure 1). From the offset of structural features and drag folds along the Keane Wonder fault, *Troxel and Wright* [1989] inferred a right-lateral or top-to-the-northwest movement. Similarly, from upper-plate field relations, *Reynolds et al.* [1986] also inferred westward movement of the upper plate.

A general southeast dip of bedding planes in the lower plate exposes progressively younger units to the southeast. Locally, dips vary across several large upright folds [*Troxel and Wright*, 1989; *Wright et al.*, 1989], a NW-SE trending anticline in the Monarch Canyon area, and a NE-SW trending syncline-anticline pair (the latter of which is the Winter's Peak anticline of *Wernicke et al.* [1988]) in the central Funeral Mountains. In the Monarch Canyon area, Late Cretaceous muscovite granite dikes inject the lower plate and comprise about 20% of the total rock package. The volume percentage decreases toward the southeast, dropping to near zero at Chloride Cliff.

Anastomosing shear zones and ductile folds pervade lower-plate rocks to the deepest observed structural levels in the northern Funeral Mountains and deform metamorphic textures inherited at high temperatures. Recent mapping [*Applegate et al.*, 1992] has found that one of the more prominent shear zones may cut out as much as 1.5 km of section. Ductile planar fabrics are oriented subparallel to the detachment fault surface. The degree of lower-temperature ductile fabric development varies locally, from intense mylonitization to almost none. Isolated pods and lenses preserve the high-temperature metamorphic texture. A resistant layer of fine-grained calc-mylonite several meters thick locally caps the exhumed surface of the Keane Wonder fault and appears to have developed during fault movement [*Hamilton*, 1988*a*]. In the central Funeral Mountains (Indian Pass area), the metamorphic texture is preserved without modification by later ductile deformation.

Metamorphism in the Funeral Mountains was a likely consequence of burial by tectonic loading. East vergent thrusts have been mapped in mountain ranges north and west of the Funeral Mountains [e.g., *Corbett et al.*, 1988; *Wernicke et al.*, 1988]. Movement along one of these, the Last Chance thrust, may have been as old as Permian [*Snow et al.*, 1991]. This suggests that sufficient time (≈100 m.y.) was available between the end of thrusting and the peak of metamorphism for heating of the thickened crust to have taken place [*England and Thompson*, 1984].

METAMORPHISM

The metamorphic petrology of lower-plate rocks provides constraints to tectonic models through determinations of pressure-temperature conditions. In examining mineral assemblages, *Labotka* [1980], *Giaramita* [1984], and *Labotka and Albee* [1988] defined a series of isograds in pelitic schis which denoted an increase in metamorphic grade to th northwest, from middle greenschist facies at Indian Pass t upper amphibolite facies at Monarch Canyon (Figure 1). Th isograds were based on an analysis of mineral assemblage using the AFM projection of *Thompson* [1957] and corre spond to specific reactions in muscovite- and quartz-bearin rocks. Isograds defined in this way are based on minera associations rather than first occurrences. Mineral assem blages from this study (Table 1) confirm these earlier studies.

Isograds based on the following two reactions were located by *Labotka* [1980] and delineate the low-grade boundaries for his "staurolite" and "kyanite" zones (names assigned by *Labotka* [1980], respectively, based on comparable zones in a Barrovian sequence; Figure 1):

(R1) staurolite + chlorite = kyanite + biotite

(R2) staurolite = garnet + kyanite + garnet.

These reactions have been located in pressure-temperature coordinates on numerous petrogenetic grids (the grid of *Spear and Cheney* [1989] is used in this study) and are thus useful in constraining the conditions of metamorphism.

Within the kyanite zone, mineral assemblages commonly comprise quartz + muscovite + biotite + garnet + kyanite + plagioclase ± staurolite ± sillimanite (Table 1*a*). The presence of staurolite in several samples (CC-34, CC-34b, CC-36, and CC-58 from Proterozoic gneiss) results either from metastable persistence or stabilization by Zn and/or Li. In the staurolite zone, mineral assemblages commonly comprise quartz + muscovite + biotite + garnet + staurolite + plagioclase (Table 1*a*). The AFM crossing tie line assemblage quartz + muscovite + garnet + kyanite + staurolite + biotite + plagioclase is common in the staurolite zone (Table 1*a*) and probably results from the stabilization of garnet by the presence of Mn and/or Ca. No difference in grade was observed between the Precambrian gneiss and the overlying Crystal Spring Formation, indicating that the Precambrian gneiss underwent total reequilibration during the metamorphism which affected the younger overlying strata.

A garnet isograd representing the first occurrence of garnet was located by *Labotka* [1980] in the Indian Pass area (Figure 1), but mineral assemblages do not constrain possible AFM continuous or discontinuous reactions responsible for the production of garnet. In the Indian Pass area, mineral assemblages typically comprise various combinations of kyanite, chloritoid, chlorite, garnet, and staurolite, with ubiquitous quartz and muscovite (*Labotka* [1980] and Table 1*b* from this study). One sample reported by *Labotka* [1980] from the Indian Pass area also contains biotite.

Samples examined in the present study from Echo Canyon, southeast of Indian Pass (inset, Figure 1), show that pelitic rocks in the lower plate comprise slates and phyllites containing quartz, muscovite, chlorite, and FeTi-oxides and are thus no higher in grade than lower greenschist facies. Upper plate pre-Tertiary rocks, including those in the Grapevine Mountains (Figure 1), are similarly low in grade.

Conditions of Metamorphism

Samples from Monarch Canyon, Chloride Cliff, and Indian Pass were analyzed for thermobarometry. Suitable samples were those which preserved equilibrium textures inherited during high-temperature metamorphism and which contained mineral assemblages applicable to calibrated thermobarometers. Undeformed metamorphic textures were rare in the Monarch Canyon, Chloride Cliff, and Keane Wonder areas owing to the pervasive nature of the lower-temperature ductile deformation; however, they were the rule in the Indian Pass area. The samples selected for analysis from the Monarch Canyon and Chloride Cliff areas preserved quartz grains with straight grain boundaries and 120° triple junctions, consistent with static recrystallization at sustained elevated temperatures. Evidence of comparatively minor subsequent lower-temperature ductile deformation is present in these samples, including kink folds in kyanite and mica grains (Figure 2), undulatory extinction in quartz, minor deformation band development, and minor grain boundary migration recrystallization in quartz. Significant grain boundary migration of minerals other than quartz did not accompany the younger deformation in these samples. The textural characteristics of these samples indicate that the arrangement of grains present during high-temperature metamorphism was preserved.

Monarch Canyon. Monarch Canyon is located within the Kyanite Zone (Figure 1). Thermobarometric methods were applied to rocks from this area by *Labotka* [1980], *Hoisch* [1989, 1990, 1991], and *Hodges and Walker* [1990], using methods applicable to rocks containing quartz, biotite, garnet, plagioclase, and kyanite. The results from *Hodges and Walker* [1990] and *Hoisch* [1991] are shown in Figure 3. In both these studies, pressures and temperatures were calculated by simultaneously solving equilibrium thermodynamic expressions for two equilibria involving mineral components in solid solution and pure stoichiometric phases, the pressure-sensitive anorthite-breakdown equilibrium (R3), and the temperature-sensitive garnet-biotite $FeMg_{-1}$ exchange equilibrium (R4):

(R3) Anorthite = Quartz + 2 Kyanite + Grossular
Plagioclase SiO_2 Al_2SiO_5 Garnet

(R4) Almandine + Phlogopite = Pyrope + Annite
Garnet Biotite Garnet Biotite.

In the thermobarometric calculations, *Hoisch* [1991] used garnet compositions measured 50–100 μm from the rims of idioblastic garnets 1.5–2.5 mm in diameter. The flat zoning profiles for these garnets (CC-33a in Figure 4) (also Figure 5 from *Hodges and Walker* [1990]) reflect homogenization and equilibration at high temperatures. Compositional gradients indicate diffusive retrograde reequilibration, with a greater degree of retrogradation at the rims than in the cores. Sample CC-36, from Proterozoic gneiss, yielded the highest temperature and pressure, 700°C at 9.1 kbar [*Hoisch*, 1991], which may be an indication that this sample is the least retrograded of those analyzed. The pressure corresponds to a depth of 32 km, assuming 0.285 kbar km^{-1}. The uncertainty in pressure using this method has been estimated to range from ±0.6 kbar to ±3.3 kbar (1σ), and the uncertainty in temperature has been estimated to be ±50°C (1σ) [*Kohn and Spear*, 1991]. Further uncertainties are introduced by a lack of knowledge of the cooling rate and of the extent of retrograde reactions [*Spear and Florence*, 1992], although the idioblastic character of the garnets suggests that there was little in the way of retrograde reactions involving garnet consumption. Some confirmation of the thermobarometry is given by the conditions associated with reaction (R2); because CC-36 comes from the kyanite zone, it should have experienced temperatures higher than (R2). The conditions determined for sample CC-36 are close to the conditions for this reaction as given by *Spear and Cheney* [1989] (710°C at 9.1 kbar).

The presence of sillimanite in Monarch Canyon (*Labotka* [1980], *Giaramita* [1984], and this study) is enigmatic in that thermobarometry indicates peak conditions compatible with kyanite instead. Sillimanite occurs in samples CC-14a, CC-14c, CC-29a (Crystal Spring Formation) and CC-58 (Proterozoic gneiss), all of which also contain kyanite (Table 1*a*). These are distributed among the many locations where

TABLE 1*a*. Mineral Assemblages With Muscovite and Quartz From Pelitic Schist in the Kyanite and Staurolite Zones

Sample	Plag	Bio	Gar	St	Ky	Sil	Op	Other[a]	Altered[b]
					Kyanite Zone				
CC-3a	x	x	x		x		x	s	Y
CC-3b	x	x	x		x		x	s	
CC-13	x	x	x		x		x	s, t	Y
CC-14a		x	x	x	x	x	x		Y
CC-14b		x	x				x		Y
CC-14c		x	x		x	x	x		Y
CC-29a		x	x		x	x	x		Y
CC-29c		x	x		x		x		
CC-29d			x		x		x	t	
CC-32	x	x	x		x		x		Y
CC-32a		x	x		x		x	t	Y
CC-32b	x	x	x		x		x	z	Y
CC-33	x	x	x		x		x	a, r, s, t, z	
CC-33a	x	x	x		x		x	a, s, z	
CC-34	x	x	x	x	x		x	t	Y
CC-34b	x	x	x	x	x		x	r, t	
CC-35	x	x	x				x	r	Y
CC-36	x	x	x	x	x		x	a, z	
CC-58	x	x	x	x	x	x	x	t	
					Staurolite Zone				
CC-5a		x	x	x			x		
CC-5b		x	x	x			x		
CC-5c		x	x	x			x		
CC-7	x	x	x	x			x		
CC-8	x	x	x	x			x		
CC-9a	x	x	x	x			x	r, t	
CC-9b		x	x	x	x		x	a, t	
CC-9c	x	x	x	x	x		x	z	Y
CC-9e	x	x	x	x			x	a, t, z	
CC-10a	x	x	x	x			x	t	Y
CC-10b	x	x	x	x			x	t	
CC-11a	x	x	x	x			x		
CC-11b	x	x	x	x			x	t	
CC-15a	x	x	x	x			x		Y
CC-15b	x	x	x	x			x	t	
CC-16a	x	x	x	x			x	a	Y
CC-16b	x	x	x	x			x	z, t	Y
CC-17b	x	x	x				x	a	Y
CC-25a	x	x	x	x	x		x	a, s	
CC-25b	x	x	x	x			x	a, z	
CC-25c	x	x	x	x			x	a, s, z	
CC-26a	x	x	x	x			x		Y
CC-26b	x	x	x	x			x	a, t, z	Y
CC-27	x	x	x	x			x		Y
CC-28a	x	x	x	x			x	t, z	Y
CC-28b	x	x	x	x	x		x	t	Y
CC-37		x		x			x	a	Y
CC-38	x	x		x			x	t	Y
CC-39	x	x	x				x	t, z	Y
CC-40a	x	x	x				x	z	Y
CC-41	x	x	x				x		
CC-61	x	x	x	x			x	r, t	
CC-72a	x	x	x	x			x	a, s, z	
CC-72b	x	x	x	x			x	a, s, t, z	
CC-72c	x	x	x	x			x	a, z	
CC-72d	x	x	x	x			x	a, t, z	
CC-74b	x	x	x	x			x	t	Y

Only primary phases are indicated. Only samples from which definitive mineral identifications could be made (i.e., sufficiently unaltered) were included. Mineral abbreviations: Bio is Biotite; Gar is Garnet; Ky is kyanite; Op is opaque oxides; Plag is plagioclase; Sil is sillimanite; St is staurolite. Sample locations are given in Figure 1.

[a]Other minerals: a is apatite; r is rutile; s is titanite; t is tourmaline; and z is zircon.

[b]Y = substantial hydrothermal alteration.

samples containing kyanite without sillimanite were found (CC-3a,b, CC-13, and CC-29c,d from the Crystal Spring Formation, and CC-32, CC-32a,b, CC-33, CC-33a, CC-34, CC-34b, and CC-36 from Proterozoic gneiss), indicating that there is no simple kyanite-sillimanite isograd [cf. *Giaramita*, 1984]. One possible interpretation is that the sillimanite was a product of retrogradation associated with cooling and decompression.

TABLE 1*b*. Mineral Assemblages With Muscovite and Quartz From Pelitic Schist in the Garnet Zone

Sample	Chte	Ky	Gar	St	Ctd	Op	Other[a]
CC-24a	x	x			x	x	t
CC-24b	x	x			x	x	t
CC-24c	x	x			x	x	t
CC-63b	x	x				x	
CC-66		x			x	x	t
CC-68b	x		x		x	x	t
CC-68c	x		x		x	x	r
CC-68g	x		x		x	x	t
CC-68i	x		x		x	x	
CC-68j	x		x		x	x	r
CC-69	x		x		x	x	t
CC-70	x		x		x	x	t
KF18[b]	x	x		x		x	a,s,z

Only primary phases are indicated. Mineral abbreviations: Chte is chlorite; Ctd is Chloritoid; Gar is Garnet; Ky is kyanite; Op is opaque oxides; and St is staurolite. Samples locations are given in Figure 1.

[a]Other minerals: a is apatite; r is rutile; s is titanite; t is tourmaline; and z is zircon.

[b]Sample provided by K. F. Fox, Jr.

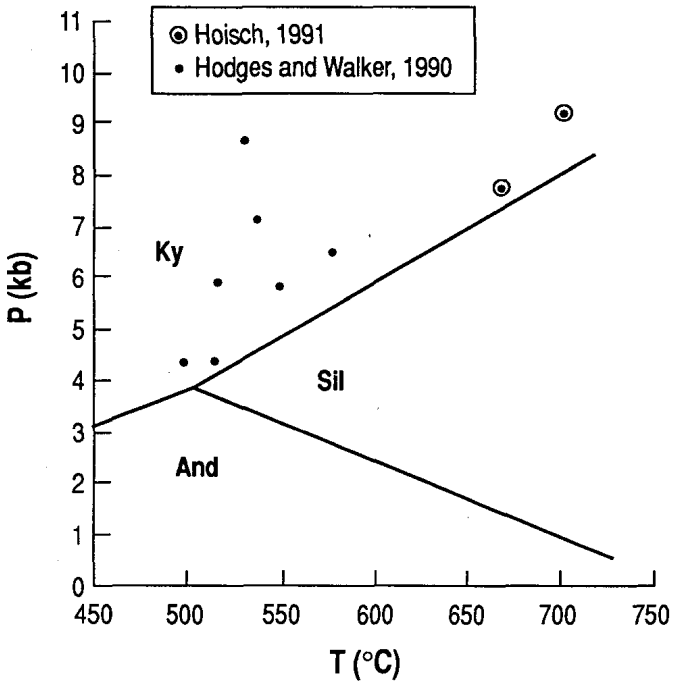

Fig. 3. Thermobarometry of rocks from Monarch Canyon using geobarometry based on the anorthite breakdown equilibrium (R3) [*Koziol and Newton*, 1988] and geothermometry based on the garnet-biotite $FeMg_{-1}$ exchange equilibrium (R4) [*Hodges and Spear*, 1982] (see discussion in text for details). Al_2SiO_5 stability fields of *Holdaway* [1971] are shown (And is andalusite, Ky is kyanite, and Sil is sillimanite).

The thermobarometric determinations by *Hodges and Walker* [1990] for samples from Monarch Canyon scatter widely (Figure 3). The variability was interpreted by them to be a product of equilibration at different points by different samples along the retrograde P-T path. It is more likely, however, that the variability is an artifact of incomplete reequilibration during retrogradation [*Frost and Chacko*, 1989; *Spear and Florence*, 1992]. It is unclear why *Hodges and Walker* [1990] obtained results different from those of *Hoisch* [1991] (Figure 3), considering that both studies used very similar calculational methods and garnet compositions measured near the rims. The isothermal decompression P-T paths determined by *Hodges and Walker* [1990] using garnet zoning and the Gibbs method of *Spear and Selverstone* [1983] are similarly problematic. None of the P-T paths calculated by *Hodges and Walker* [1990] pass through the sillimanite stability field and the highest temperature reached along the paths is 634°C. The occurrence of sillimanite and the achievement of temperatures above (R2) (≈710°C at 9.1 kbar according to *Spear and Cheney* [1989]) are inconsistent with the P-T paths.

Chloride Cliff. Chloride Cliff is located within the staurolite zone (Figure 1). Thermobarometry from four samples

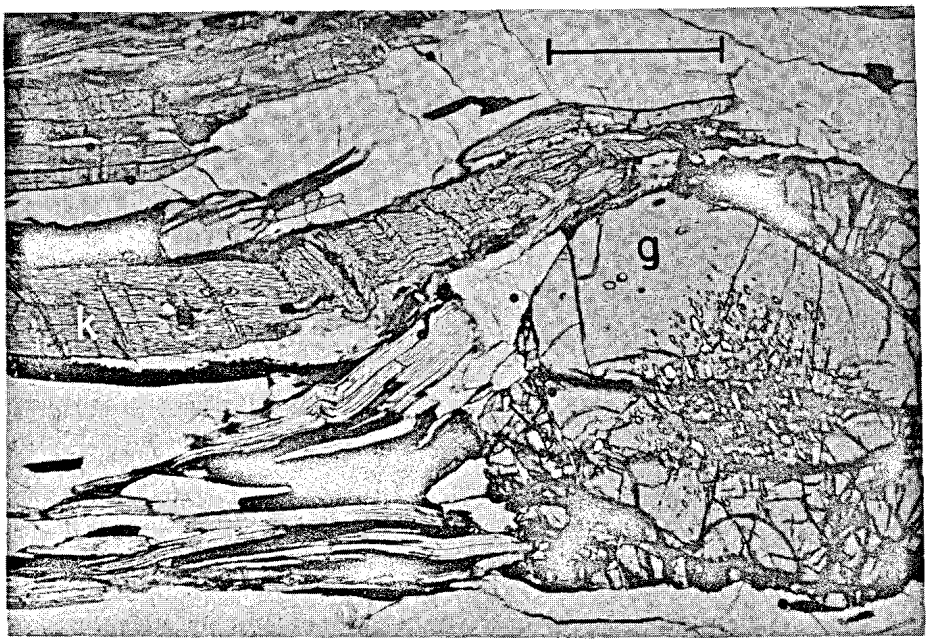

Fig. 2. Kink folds in kyanite (k) buttressed by a garnet (*g*) crystal, from sample CC-32a (Monarch Canyon, location in Figure 1). Plane-polarized light. Scale bar is 1 mm long.

is plotted in Figure 5, having been calculated using mineral composition data from Table 2 (CC-72b, CC-72c, CC-72d, Kingston Peak Formation) and from *Hoisch* [1990] (CC-25c, Kingston Peak Formation) using geobarometry [*Hoisch*, 1991] based on 43 fluid-independent equilibria calibrated empirically against the anorthite breakdown geobarometer (R3) [*Koziol and Newton*, 1988], and geothermometry based on the garnet-biotite $FeMg_{-1}$ exchange equilibrium (R4) [*Hodges and Spear*, 1982]. Garnets representing a range of sizes (1.5–3.9 mm in diameter) were analyzed about 100 μm from the rims. These samples lack any Al_2SiO_5 phase but contain the minerals quartz, muscovite, biotite, garnet, and plagioclase, which are necessary for application of the geobarometers used. Garnets in these samples are embayed around the rims, probably as a result of consumption during prograde staurolite growth. Flat composition profiles for small garnets (CC-25c in Figure 4) and symmetrical growth-zoning profiles [e.g., *Tracy*, 1982] for large garnets (CC-72d in Figure 4) indicate that temperatures were not high enough or insufficiently sustained to homogenize the larger garnets.

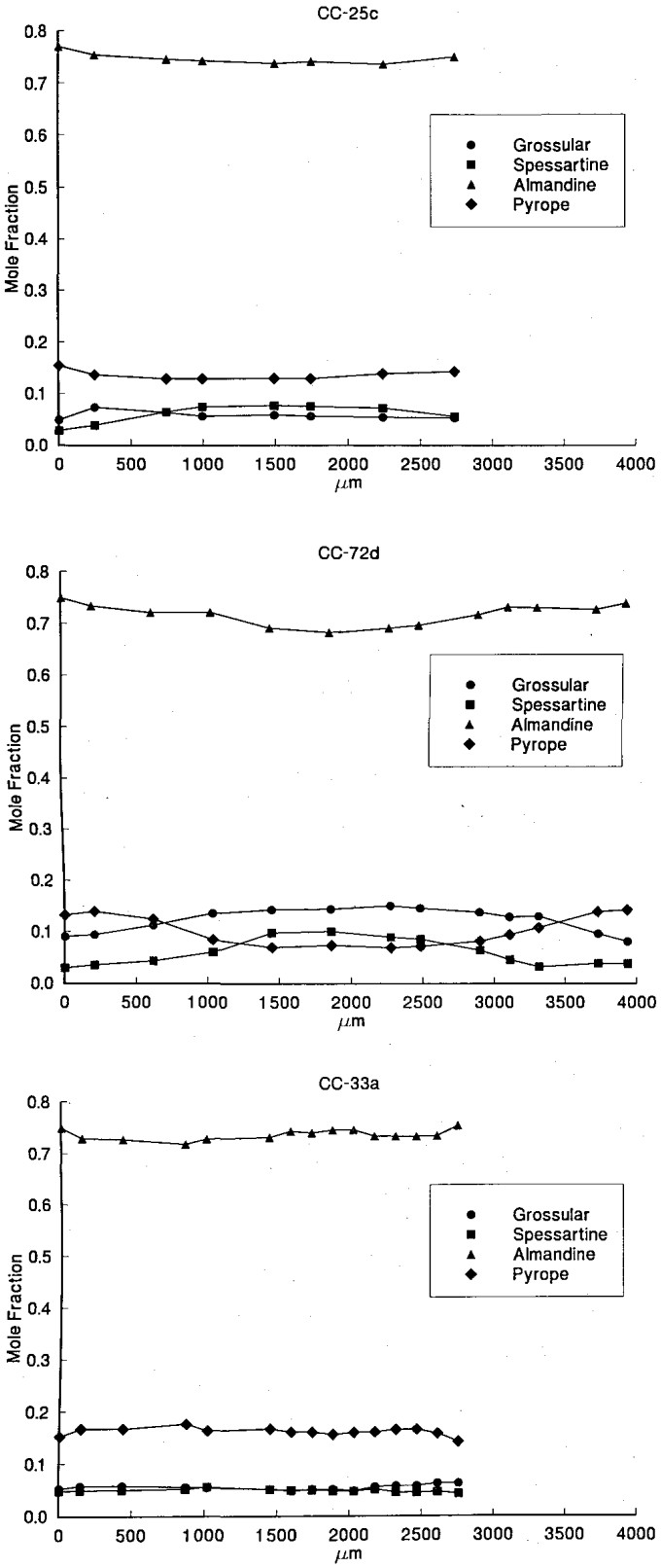

Fig. 4. Zoning profiles for garnets from samples of pelitic schist. Endpoints are 50–100 μm from the garnet rims. CC-33a is from the bottom of Monarch Canyon (Proterozoic gneiss), and both CC-25c and CC-72d are from Chloride Cliff (Kingston Peak Formation, locations in Figure 1). See text for discussion.

In each diagram of Figure 5, the intersection of the near-vertical line, which represents the garnet-biotite geothermometer (R4), with the other more gently sloping lines, which represent the 43 fluid-independent equilibria, indicate the conditions of metamorphism. Only these intersections are significant because the method used to calibrate the 43 equilibria involved fitting them to an empirical data set in which the P-T conditions were determined from the intersection of (R3) by (R4). The intersections in the diagrams indicate temperatures of 575°–600°C and pressures of 5.5–7.7 kbar (19–27 km depth). Because these geobarometers were calibrated against the anorthite-breakdown geobarometer (R3), they inherit the uncertainties associated with it discussed by *Kohn and Spear* [1991].

The temperatures and pressures determined in samples from Chloride Cliff (Figure 5) show less scatter than the higher-temperature rocks from Monarch Canyon (Figure 3). This conforms to the notion of less retrogradation at Chloride Cliff, which is to be expected because volume diffusion in garnet becomes sluggish at temperatures below ≈600°C [e.g., *Spear*, 1989]. This is also consistent with the homogenization of small garnets but not large garnets at Chloride Cliff.

Indian Pass and the Southern Funeral Mountains. On sample CC-68b, Johnnie Formation from the Indian Pass area, geothermometry based on the garnet-chlorite $FeMg_{-1}$ exchange equilibrium [*Grambling*, 1990] was applied using mineral composition data from Table 2 (Figure 6). The garnet composition was measured approximately 50 μm from the rim of an idioblastic garnet 1.2 mm in diameter. A temperature of 490 ± 50°C was calculated. Although sample CC-68b does not contain kyanite, it is common in the Indian Pass area (*Labotka* [1980] and Table 1*b*). This places a lower pressure limit of 3.6 kbar on the conditions of metamorphism (Figure 6).

From the southern Funeral Mountains, about 50 km southeast of Monarch Canyon, two determinations of conodont color alteration index were reported by *Harris et al.* [1980]; one yielded a value of 5 and the other a value of 6, both from Devonian units. These indicate temperatures in the range 325°–425°C or low-greenschist to subgreenschist facies conditions, assuming a long heating duration of 10–100 m.y. [*Rejebian et al.*, 1987]. Because these are lower temperatures than recorded at Indian Pass, they are consistent with the regional trend of decreasing metamorphic grade to the southeast.

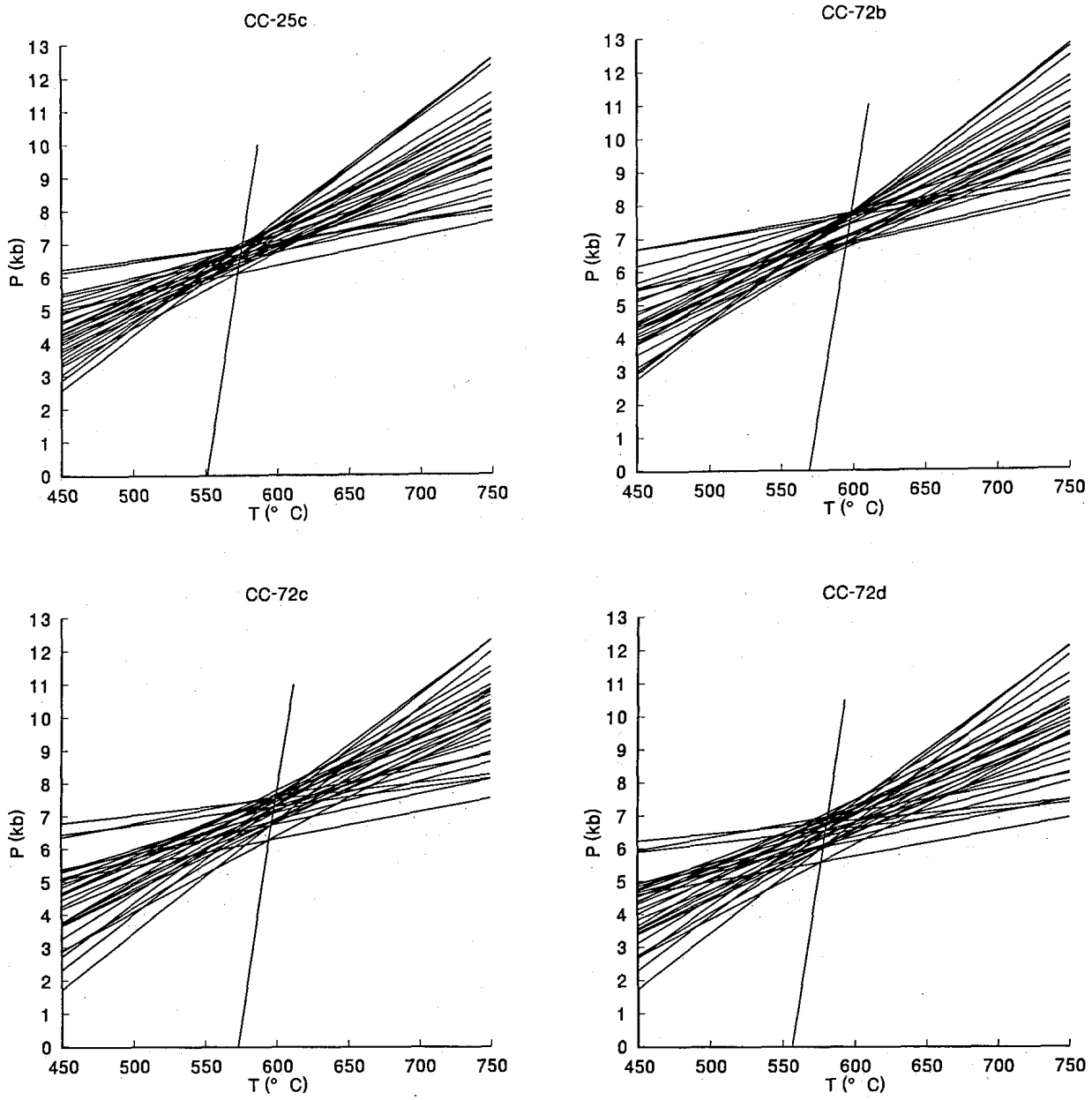

Fig. 5. Thermobarometry from four samples from Chloride Cliff, calculated using data from Table 2 for CC-72b, CC-72c, and CC-72d, and from *Hoisch* [1990] for CC-25c (all from same outcrop, location in Figure 1). Plotted are 43 geobarometers [*Hoisch*, 1991], and the garnet-biotite geothermometer (R4) (near-vertical line) [*Hodges and Spear*, 1982].

Hydrothermal Alteration

Hydrothermally altered minerals are widespread throughout the northern Funeral Mountains. Commonly, staurolite and folded kyanite grains are altered to sericite, and garnet is altered to chlorite (Figure 7). As noted by *Labotka* [1980], the alteration is strongest in a zone extending from the Keane Wonder Mine visitor parking area to Chloride Cliff, then trending northwest along the Boundary Canyon fault. Unaltered rocks are, however, locally found within the zone of extensive alteration (e.g., at location CC-25/61/72).

FABRIC DEVELOPMENT

High-Temperature Fabrics

Only a small percentage of the samples collected in the northern Funeral Mountains preserved the high-temperature metamorphic texture without substantial modification by lower-temperature ductile deformation. Consequently, a systematic study of the high-temperature fabric was not possible. All samples analyzed for thermobarometry in this study (Figures 5 and 6) and by *Hoisch* [1991] (plotted in Figure 3 in this study) were among those which preserved the high-temperature metamorphic texture with little or no lower-temperature modification.

Sample CC-59a, a garnet amphibolite (metamorphosed basaltic dike) from Proterozoic gneiss at the bottom of Monarch Canyon (location in Figure 1), displays a texture that is particularly illustrative of inheritance at or near the peak of metamorphism. Hornblende crystals have average dimensions of 2.5 × 0.25 × 0.35 mm and are strain-free. Equidimensional plagioclase and quartz grains of ≈0.25-mm diameter have planar or gently curved boundaries that truncate against amphiboles, indicative of extensive grain boundary migration recrystallization [*Urai et al.*, 1986].

TABLE 2*a*. Muscovite Analyses in Weight Percents of the Oxides

	CC-72b	CC-72c	CC-72d
Average of	3	3	2
F	0.00	0.00	0.00
Na_2O	2.18	1.66	1.71
MgO	0.56	0.65	0.66
Al_2O_3	36.20	33.43	34.61
SiO_2	47.35	45.89	46.01
K_2O	7.60	8.11	8.16
CaO	0.00	0.03	0.01
TiO_2	0.47	0.41	0.44
MnO	0.04	0.00	0.04
FeO[a]	0.90	2.46	2.30
Total	95.30	92.64	93.92
Formulas Based on 11 Oxygens			
F	0.00	0.00	0.00
Na	0.28	0.22	0.22
Mg	0.05	0.07	0.07
Al	2.79	2.69	2.74
Si	3.10	3.13	3.09
K	0.64	0.71	0.70
Ca	0.00	0.00	0.00
Ti	0.02	0.02	0.02
Mn	0.00	0.00	0.00
Fe^{2+}	0.05	0.14	0.13

[a]All Fe as Fe^{2+}.

TABLE 2*c*. Garnet Analyses in Weight Percents of the Oxides

	CC-72b	CC-72c	CC-72d	CC-68b
Average of	4	4	1	2
Na_2O	0.00	0.00	0.09	0.00
MgO	3.75	3.47	3.35	1.86
Al_2O_3	21.35	21.15	21.26	21.38
SiO_2	38.17	38.25	38.19	37.97
K_2O	0.01	0.00	0.00	0.01
CaO	1.98	3.49	3.18	2.96
TiO_2	0.01	0.02	0.04	0.05
MnO	1.36	1.32	1.30	5.12
FeO[a]	34.94	33.70	33.92	33.09
Fe_2O_3[a]	0.53	0.30	0.96	0.00
Total	102.09	101.69	102.30	102.43
Formulas Based on 12 Oxygens and 8 Cations[a]				
Na	0.00	0.00	0.01	0.00
Mg	0.44	0.41	0.39	0.22
Al	1.98	1.96	1.96	1.99
Si	3.00	3.01	2.99	3.00
K	0.00	0.00	0.00	0.00
Ca	0.17	0.29	0.27	0.25
Ti	0.00	0.00	0.00	0.00
Mn	0.09	0.09	0.09	0.34
Fe^{2+}	2.30	2.22	2.22	2.19
Fe^{3+}	0.03	0.02	0.06	0.00

[a]Calculated through simultaneous normalization to 12 oxygens and 8 cations. Normalization of 12-oxygen with all Fe as Fe^{2+} took precedence if 8-cation constraint could not be met.

Some quartz grains preserve deformation bands, but all show full recovery of intracrystalline strain. The sample also contains polycrystalline aggregates of titanite, 6 × 0.9 mm, minor iron oxide, quartz, and epidote, which help define the mineral lineation along with individual 0.180 × 0.090 mm titanite grains and hornblende. Poikiloblastic garnets have overgrown aligned titanite, hornblende, and elongate quartz grains that are oblique to the main foliation by 35°–45°. A subset of hornblende grains in the matrix also lies at ≈39° to the main fabric. The oblique fabrics, both in the matrix and within the garnets, curve into parallelism with the main foliation, and the rock is interpreted to be a high-temperature *S-C* mylonite [*Berthé et al.*, 1979], in which syntectonic titanite and amphibole growth occurred on both *S* and *C* planes. Prograde metamorphism, involving garnet growth and recovery of internal strain in the rock, postdated most of the deformation. A similar composite fabric is observed in metapelite sample CC-58 (basement gneiss), in which the *S* and *C* planes are defined by recrystallized biotite and kyanite (Figure 8).

TABLE 2*b*. Biotite Analyses in Weight Percents of the Oxides

	CC-72b	CC-72c	CC-72d
Average of	3	3	3
F	0.15	0.12	0.11
Na_2O	0.28	0.36	0.44
MgO	11.10	11.41	11.49
Al_2O_3	19.34	18.45	18.63
SiO_2	37.26	37.18	37.03
K_2O	8.32	8.50	8.19
CaO	0.00	0.01	0.03
TiO_2	1.87	1.61	1.73
MnO	0.06	0.02	0.00
FeO[a]	17.70	18.22	18.31
Total	96.01	95.84	95.91
Formulas Based on 11 Oxygens			
F	0.03	0.03	0.03
Na	0.04	0.05	0.06
Mg	1.23	1.27	1.27
Al	1.69	1.62	1.63
Si	2.76	2.77	2.76
K	0.79	0.81	0.78
Ca	0.00	0.00	0.00
Ti	0.10	0.09	0.10
Mn	0.00	0.00	0.00
Fe^{2+}	1.10	1.14	1.14

[a]All Fe as Fe^{2+}.

TABLE 2*d*. Plagioclase Analyses in Weight Percents of the Oxides

	CC-72b	CC-72c	CC-72d
Average of	2	3	3
Na_2O	9.86	8.01	8.07
MgO	0.00	0.00	0.01
Al_2O_3	23.48	25.89	25.88
SiO_2	64.83	60.71	60.96
K_2O	0.05	0.04	0.03
CaO	3.98	6.91	6.99
TiO_2	0.00	0.00	0.00
MnO	0.00	0.00	0.00
FeO[a]	0.03	0.02	0.09
Total	102.23	101.59	102.03
Formulas Based on 8 Oxygens			
Na	0.83	0.68	0.68
Mg	0.00	0.00	0.00
Al	1.20	1.34	1.33
Si	2.80	2.66	2.66
K	0.00	0.00	0.00
Ca	0.18	0.32	0.33
Ti	0.00	0.00	0.00
Mn	0.00	0.00	0.00
Fe^{2+}	0.00	0.00	0.00

[a]All Fe as Fe^{2+}.

TABLE 2e. Chlorite Analysis in Weight Percents of the Oxides

	CC-68b
Average of	2
Na_2O	0.03
MgO	13.14
Al_2O_3	23.06
SiO_2	24.36
K_2O	0.09
CaO	0.02
TiO_2	0.07
MnO	0.16
FeO[a]	27.20
Total	88.12
Formula Based on 8 Oxygens	
Na	0.01
Mg	2.07
Al	2.88
Si	2.58
K	0.01
Ca	0.00
Ti	0.01
Mn	0.01
Fe^{2+}	2.41

[a]All Fe as Fe^{2+}.

Of 23 oriented samples taken from areas throughout the northern Funeral Mountains, four samples preserved the high-temperature fabric relatively unaffected by the lower-temperature deformation, but only two of these preserved high-temperature rotational strain indicators; sample CC-59a indicated top-to-the-southwest (toward 241°, parallel to a mineral lineation which plunges 18° toward 61°) and sample CC-58 indicated top-to-the-northwest (toward 331°, parallel to a mineral lineation which plunges 19° toward 151°). The shear senses bear no clear relationship to those recorded within lower-temperature fabrics (discussed below) and are themselves contradictory.

Low-Temperature Ductile Deformation Fabrics

Conditions of Mylonitization. The grain size in a quartz mylonite places limits on the temperature at the time that dynamic recrystallization ended. Progressive misorientation of subgrains to form new grains during deformation (rotation recrystallization [*Poirier and Nicolas*, 1975]) results in a reduction of grain size [*Twiss*, 1977; *Edward et al.*, 1982]. Concurrent grain boundary migration may either increase or decrease the grain size [e.g., *Zeuch*, 1983]. Once grain size reduction ends, growth occurs under conditions of sustained elevated temperatures, driven by surface energy reduction [*Urai et al.*, 1986]. Experimental treatments of grain growth kinetics in novaculite and flint [*Tullis and Yund*, 1982; *Pierce and Christie*, 1987] show that below certain threshold temperatures, grain growth becomes too slow to cause a significant enlargement. In order to investigate the lowest temperature at which mylonitization ended, the sample preserving the smallest grain size was used in the following analysis.

The smallest grain size in a quartz mylonite, 50-μm average diameter, was found in a sample near the bottom of Monarch Canyon (CC-1b from the Crystal Spring Formation; Figure 9). Because grain growth may have occurred after mylonitization ended, the initial grain size must have been $\leq$50 μm. Figure 10 shows the evolution of quartz grain sizes predicted by a numerical integration of the growth function of *Pierce and Christie* [1987] assuming a cooling rate of 4°C m.y.$^{-1}$, starting temperatures of 470° and 500°C, and initial grain diameters of 10, 20, and 30 μm. The model predicts that upon cooling, the final grain size will be about 50 μm when the initial grain sizes are inherited (mylonitization ends) at 470°C. The model further predicts that the final grain size will be about 130 μm when the initial grain sizes are inherited at 500°C. The fact that the initial grain size is not independently known poses little problem because the results are insensitive to the assumed values (Figure 10). The assumed cooling rate also has little influence on final grain sizes. In a model using a cooling rate of 8°C m.y.$^{-1}$, but otherwise identical to Figure 10, a final grain size of about 50 μm is achieved when the initial grain sizes are inherited at 480°C. Thus it appears likely that grain size reduction in CC-1b ended at temperatures below about 470°–480°C.

A lower temperature limit for the end of dynamic recrystallization is given by limits of ductility in quartz. Experimental studies have shown that dislocation glide and climb freeze below about 250°–300°C in hydrolytically weakened quartz [*Tullis and Yund*, 1980]. In CC-1b, the optically strain-free character of dynamically recrystallized grains, their organization into elongate subgrains and new grains, and the gentle curvature of their grain boundaries, imply a level of efficiency in recovery processes such as climb, which requires temperatures significantly above the critical minimum. Thus we consider that dynamic recrystallization in sample CC-1b ended at temperatures above 325°C.

Kinematics of Low-Temperature Ductile Deformation. Determinations of shear sense in the lower-temperature microfabrics were made using asymmetric porphyroclasts [*Passchier and Simpson*, 1986], shear bands [*Berthé et al.*, 1979] (Figure 11*a*), mica fish [*Lister and Snoke*, 1984] (Figure 11*a*), grain shape preferred orientations, and crystallographic preferred orientations [*Simpson and Schmid*, 1983] (Figure 12). Of the 23 oriented samples collected, 18

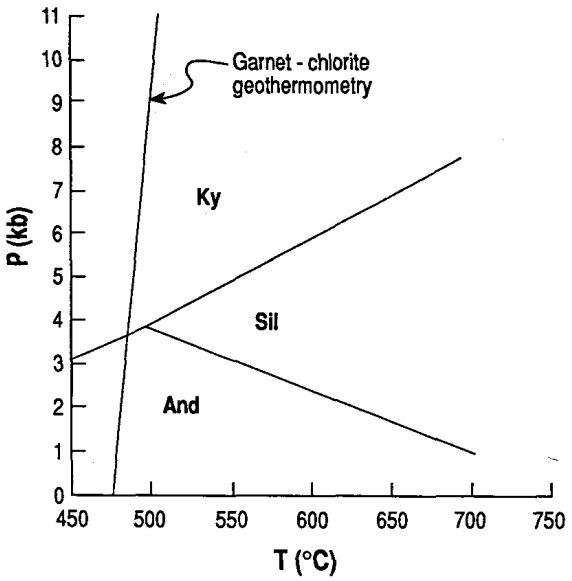

Fig. 6. Garnet-chlorite geothermometry from Indian Pass, sample CC-68b (location in Figure 1), calculated using data from Table 2 and the calibration of *Grambling* [1990]. The presence of kyanite in nearby samples (Table 1*b* and *Labotka* [1980]) restricts pressures to greater than 3.6 kbar. Al_2SiO_5 stability fields from *Holdaway* [1971] are shown. And is andalusite, Ky is kyanite, and Sil is sillimanite.

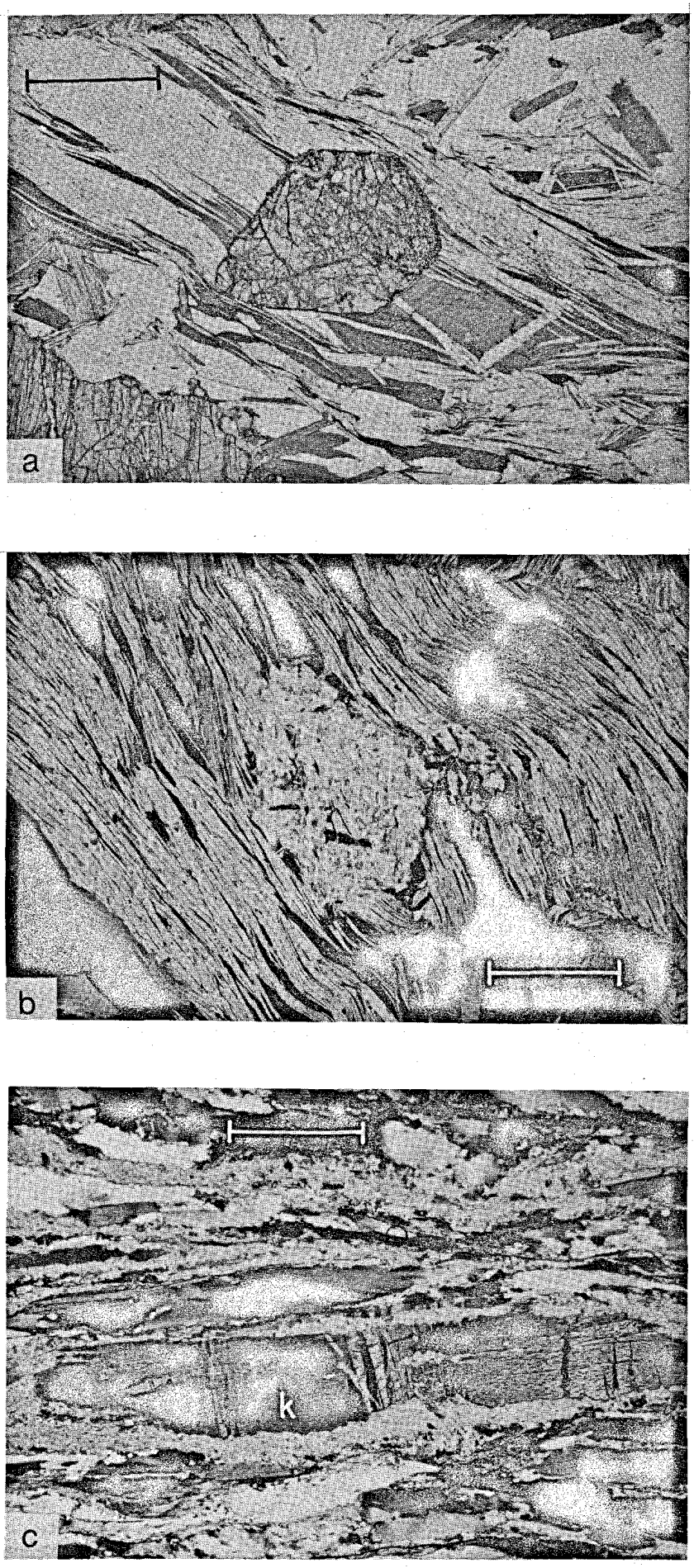

Fig. 7. Photomicrographs of pelitic schist showing examples of hydrothermal alteration. Scale bars are 1 mm long. (*a*) Fresh staurolite (center) from CC-25b (Chloride Cliff, location in Figure 1). Plane-polarized light. (*b*) Sericitic alteration of staurolite crystal from CC-37 (Keane Wonder Mine visitor parking area, location in Figure 1), showing well-preserved outline. Cross-polarized light. (*c*) Sericitic alteration of a kink-folded kyanite grain (k) in CC-32b (Monarch Canyon, location in Figure 1); sericite is distributed along shear planes. Cross-polarized light.

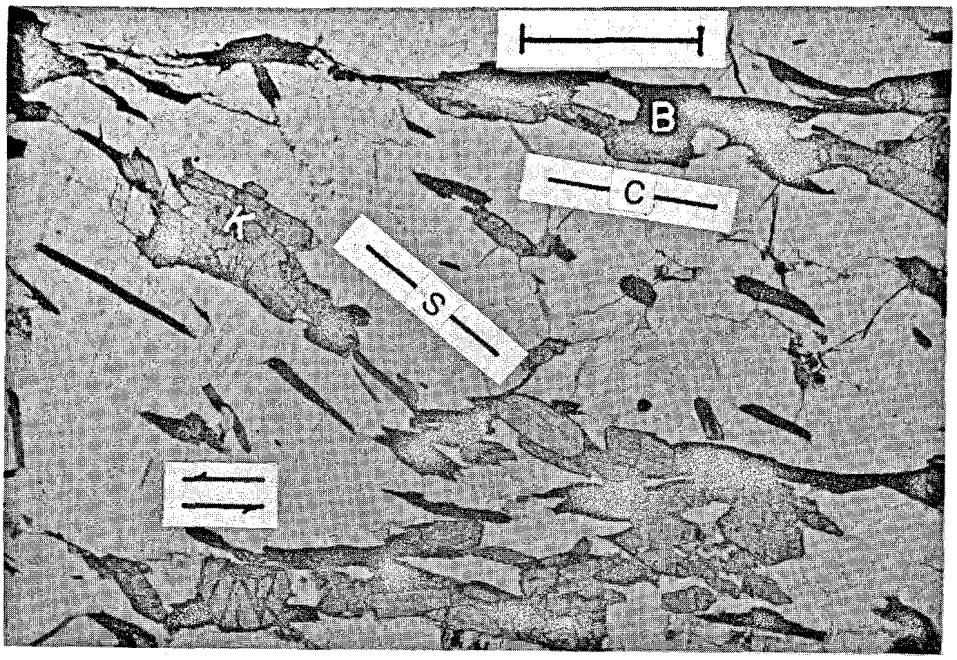

Fig. 8. Photomicrograph of sample CC-58 (Monarch Canyon, location in Figure 1), pelitic schist preserving high-temperature texture. Section is cut parallel to lineation (19° toward 151°) and perpendicular to foliation. A high-temperature *S-C* fabric denotes sinistral (top to the northwest, toward 331°) shear. Scale bar is 1 mm long. Plane-polarized light. Two planar surfaces (*S* and *C*) are marked. B is biotite, and K is kyanite.

preserved well-developed low-temperature fabrics, and of these, 11 preserved unambiguous rotational strain indicators. These 11 samples were collected from several areas in the northern Funeral Mountains within 300 m structurally below the detachment fault (bottom of Monarch Canyon, Keane Wonder Mine visitor parking area, and along the Boundary Canyon fault), and indicate that upper surfaces moved toward 299° ± 12° (top to the northwest) relative to lower surfaces (Figure 13). Mesoscale asymmetric porphyroclasts (Figure 14) are also consistent with this movement direction. Figure 11*a* shows one good example of a microfabric containing clear rotational strain indicators in a deformed Late Cretaceous muscovite granite from a location near the bottom of Monarch Canyon (sample CC-56). The sample contains well-developed shear bands and large muscovite "fish" [cf. *Lister and Snoke*, 1984]. Quartz shows a grain shape preferred orientation of elongate, straight-sided grains and subgrains with very little undulatory extinction.

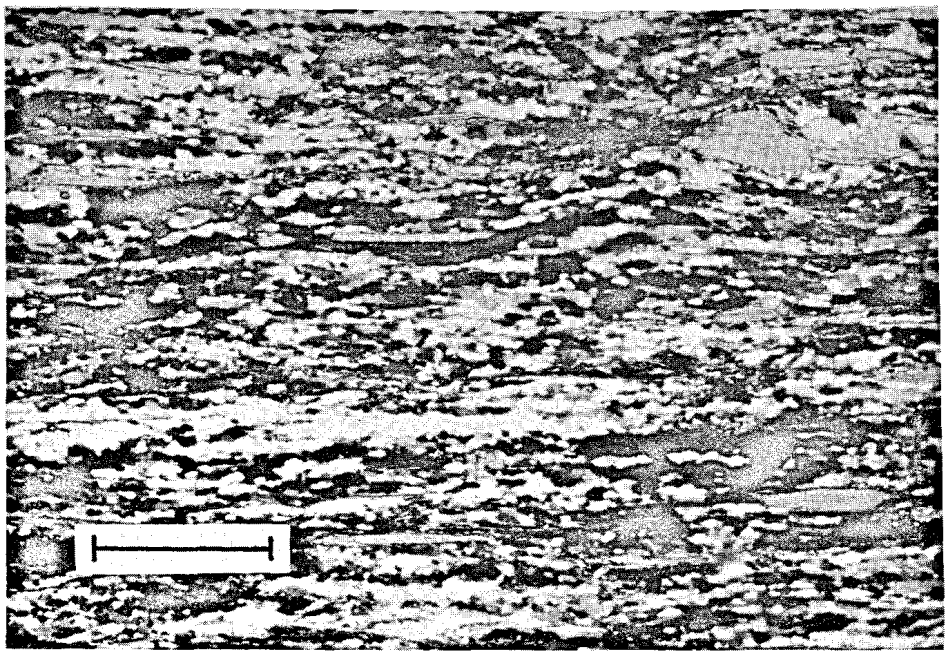

Fig. 9. Photomicrograph of sample CC-1b (from south of Monarch Canyon along southwestern flank of range, location in Figure 1), which is the finest-grained quartz mylonite found in the Funeral Mountains in this study. Cross-polarized light. Scale bar is 0.5 mm long. Section is cut parallel to lineation and perpendicular to foliation. Sample is unoriented.

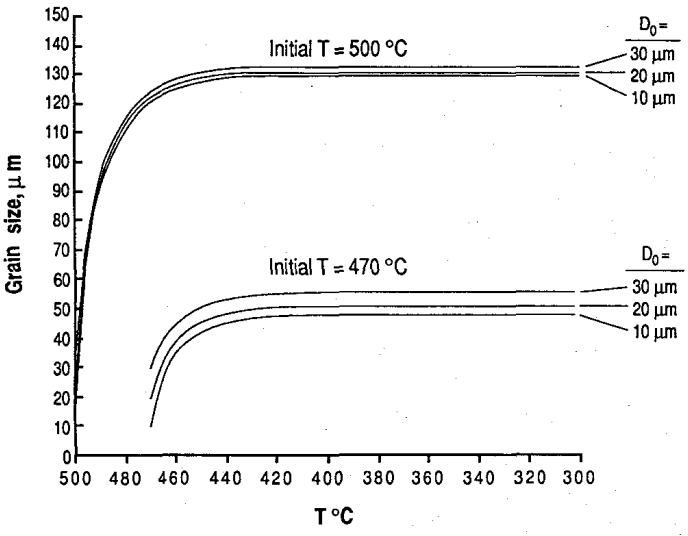

Fig. 10. Static growth curves for a quartz rock of initial average grain size D_0. Three different initial grain sizes are assumed (D_0 = 10, 20, and 30 μm), and two different starting temperatures for growth are assumed, 470° and 500°C. Curves are calculated numerically using the growth function of *Pierce and Christie* [1987] in combination with an assumed cooling rate of 4°C m.y.$^{-1}$.

Feldspar commonly contains quartz-filled extension cracks (Figure 11*b*), and also shows evidence for strain removal of twins and rotation recrystallization in the vicinity of *C* planes. Newly recrystallized 10–30-μm diameter feldspar grains and subgrains are irregular in outline, which suggests components of grain boundary migration recrystallization and rotation recrystallization.

Calc-mylonite samples were collected from the Keane Wonder Mine visitor parking area where they cap the exhumed surface of the Keane Wonder fault (location CC-50) and from the lower plate near the Boundary Canyon fault (locations CC-53 and CC-54). The calc-mylonites comprise >95% calcite of grain sizes of 20–50 μm, which is strongly reduced from the initial grain size of >4 mm (the grain size of nonmylonitic calcite marbles). All have mesoscopic foliations and lineations defined by color bands and by thin trails of opaque minerals. The high proportion of twinned grains suggests that deformation occurred within the calcite twinning regime (lower greenschist facies [*Schmid et al.*, 1987]). Calcite *C* axes in sample CC-50 show a strong point maximum close to the foliation normal (Figure 12), with an asymmetry that is consistent with the shear sense determined from oblique grain-shape fabrics. The low angle between the foliation normal and the point maximum suggests only a small component (20%) of simple shear, the balance being pure shear [*Wenk et al.*, 1987]. The large component of pure shear is somewhat anomalous, in that the distribution of calc-mylonites along the fault surface suggests that they developed contemporaneous with fault movement [*Hamilton*, 1988*a*] and involved a large component of simple shear. Because grain growth in calcite aggregates is faster than quartz aggregates [*Tullis and Yund*, 1982], it can be inferred that grain size reduction in the calc-mylonites ended at lower temperatures than quartz mylonites of comparable average grain size (e.g., sample CC-1b, Figure 9).

The top-to-the-northwest transport direction determined from low-temperature ductile microfabrics (Figure 13) is consistent with the direction determined from 14 measurements of fold axes and overturning directions in asymmetric tight to isoclinal folds using the arc-separation technique of *Hansen* [1971] (Figure 15). A northwest vergence was also determined by *Applegate et al.* [1992] for their F_4 generation folds, the same fold generation measured in this study. Asymmetric ductile folds are most common in interlayered marbles, calc-schists, and pelitic schists within the lower plate, but several were found in calc-mylonites at the Keane Wonder Mine visitor parking area, where the shear fabric is axial planar to the folds. In the latter area and locally in Monarch Canyon, fold axes parallel the movement direction, consistent with rotation toward the finite stretch direction at high shear strains. This suggests that the development of these folds was broadly synchronous with the development of planar shear fabrics (S_3 of *Applegate et al.* [1992]). Like the planar shear fabrics, northwest vergent folds probably developed over a range of temperatures.

Brittle Fabrics of Near-Surface Deformation

Along the contact with the Boundary Canyon fault at location CC-54, cataclasis in dolomite and quartzite (samples CC-54b and CC-54c from the Stirling Quartzite, Figure 16), and optically strained quartz lacking visible subgrains, record brittle or semibrittle behavior at temperatures and confining pressures below, or at strain rates above, those of the quartz mylonites and calc-mylonites. These may be interpreted to be products of strain at near-surface conditions associated with fault movement. The cataclastic fabrics yielded no independent indication of movement direction. *Reynolds et al.* [1986] inferred a top-to-the-west movement direction in the interval 9–5 Ma from field relations and geochronology in upper-plate rocks. This interval largely coincides with rapid cooling of the lower plate through 285°–120°C from 11–6 Ma [*Holm and Dokka*, 1991]. Through most of this interval, quartz should have been behaving brittley [*Tullis and Yund*, 1982]. Thus like the ductile deformation fabrics, the brittle deformation fabrics also developed during generally westward movement of the upper plate.

COOLING HISTORY FROM $^{40}Ar/^{39}Ar$, CONVENTIONAL K-Ar, AND FISSION TRACK DATA

The cooling history of lower-plate metamorphic rocks was investigated using $^{40}Ar/^{39}Ar$ methods applied to muscovite, biotite, and hornblende by *DeWitt et al.* [1988], and using fission track methods applied to zircon, titanite, and apatite by *Holm and Dokka* [1991]. Additionally, the present study reports conventional K-Ar data for muscovite, biotite, and hornblende (Table 3), one $^{40}Ar/^{39}Ar$ analysis of hornblende (Figure 17), and one fission track apatite analysis (Table 4). *DeWitt et al.* [1988] concluded that the peak of metamorphism was reached in Early Cretaceous time, with cooling below the muscovite closure temperature occurring at about 55 Ma near Chloride Cliff and in late Early Cretaceous (Albian) time in lower-grade areas several kilometers to the south and southeast. This interpretation was complicated by extreme problems with contamination by excess ^{40}Ar, which causes erroneously old ages.

The hornblende sample analyzed by the $^{40}Ar/^{39}Ar$ method in this study (CC-42, Figure 17) is from an undeformed garnet amphibolite (metamorphosed basaltic dike) within the

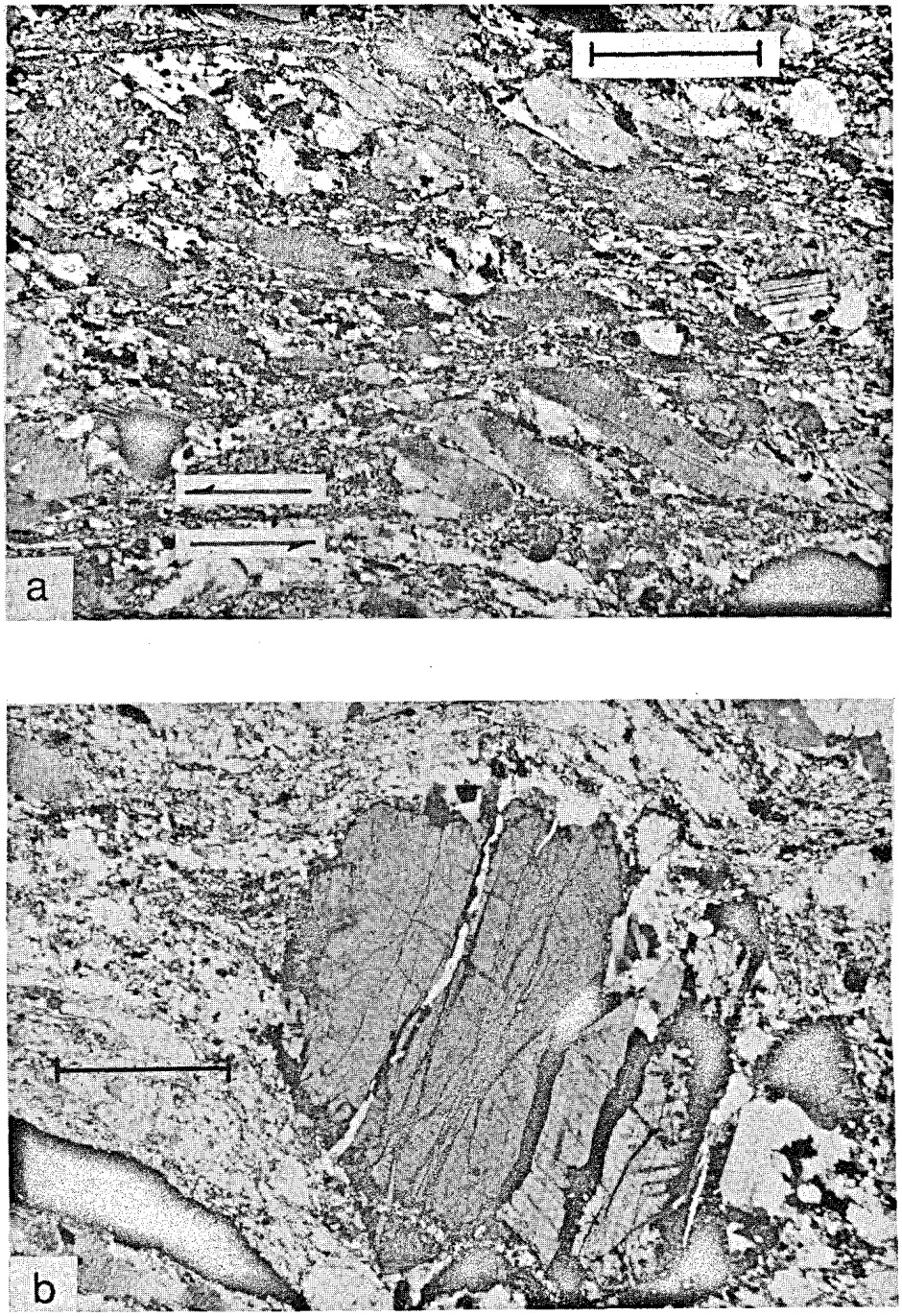

Fig. 11. Photomicrographs of deformed muscovite granite sample CC-56 (Monarch Canyon, location in Figure 1). Scale bars are 1 mm long; cross-polarized light. (*a*) Well-developed shear bands and mica fish record sinistral (top-to-the-northwest, toward 314°) movement paralleling the stretching lineation which plunges 6° toward 314°. (*b*) Cracked plagioclase; cracks are stable (do not extend into the matrix) and are filled with quartz (discussed in text).

Kingston Peak Formation near Chloride Cliff (location in Figure 1). The lowest-temperature (750°C) increment yielded an anomalously high age; the next four increments (850°, 950°, 1000°, 1100°C) produced a largely flat profile and yielded a weighted mean plateau age of 112.9 ± 0.8 Ma. Because anomalously old ages were obtained from even the flat portions of some hornblende spectra in E. DeWitt's data set (unpublished data, personal communication to T. D. Hoisch, 1987), this age should be regarded as a maximum.

Conventional K-Ar determinations have been carried out on muscovite, biotite, and hornblende from the Monarch Canyon and Keane Wonder Mine visitor parking areas (data in Table 3, sample locations in Figure 1). From Monarch Canyon, muscovite ages of 21.0 and 43.8 Ma were determined from Proterozoic gneiss (82-38, CC-58), and 62.7 Ma from Johnnie Formation (JN85CC-4). Biotite from the same two samples of Proterozoic gneiss yielded 21.3 Ma and 73.9 Ma, respectively. A third sample from the Proterozoic gneiss (82-39) yielded 50.8 Ma on biotite and 67.4 Ma on hornblende. A hornblende sample (JN85CC-3) from the Johnnie Formation yielded 543.2 Ma. Samples 82-38, 82-39, and CC-58 came from deep structural levels (>500 m) beneath the detachment fault, and samples JN85CC-3 and JN85CC-4 came from a few tens of meters beneath the fault. The ages for a specific mineral show no correlation with structural depth; the variability probably resulted from the excess ^{40}Ar

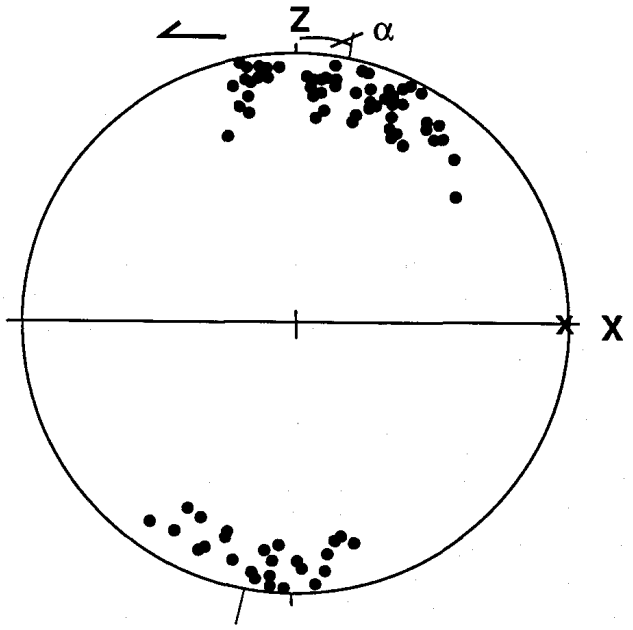

Fig. 12. Lower-hemisphere equal area projections of calcite *C* axes from calc-mylonite sample CC-50 (Keane Wonder Mine visitor parking area, location in Figure 1). Sample is oriented with lineation horizontal and foliation plane vertical. "Z" is the pole to foliation. The small angle α between *C* axis maximum and pole to foliation plane suggests a low component of simple shear [*Wenk et al.*, 1987]. Movement direction (top-to-the-northwest, toward 280°) is parallel to the stretching lineation which plunges 19° toward 280°, consistent with that indicated by the oblique grain shape fabric in the same sample.

problems discussed by *DeWitt et al.* [1988]. Excess ^{40}Ar may also have affected K-Ar ages for muscovite, biotite, and hornblende obtained from samples of Crystal Spring Formation (JN85CC-1, JN85CC-2) near the Keane Wonder Mine visitor parking area: 48.3, 50.9, and 133.6 Ma, respectively.

If the variability in ages for a specific mineral in a specific location is due to problems with excess ^{40}Ar, then the minimum age obtained should provide a meaningful maximum age constraint. Accordingly, passage through biotite, muscovite, and hornblende closure temperatures in Monarch Canyon occurred after 21, 21, and 67 Ma, respectively. In the combined Chloride Cliff and Keane Wonder areas, passage through closure temperatures occurred after 48, 51, and 113 Ma. Plateau ages from DeWitt's $^{40}Ar/^{39}Ar$ data set (unpublished data) are either similar to or older than these for the respective areas. Ar-closure temperatures have been estimated to be ≈300–350°C for biotite, ≈350°C for muscovite, and ≈500°C for hornblende [*McDougall and Harrison*, 1988].

Using fission track analysis, *Holm and Dokka* [1991] reported ages of 9.0 ± 2.6 Ma on titanite, 10.6 ± 1.6 Ma on zircon, and 6.6 ± 3.0 Ma on apatite, from deformed Late Cretaceous muscovite granite in Monarch Canyon. From Chloride Cliff, apatite from pelitic schist sample CC-61 (Kingston Peak Formation) yielded an age of 5.6 ± 1.4 Ma (this study, Table 4). Closure temperatures are approximately 285°C for titanite [*Harrison et al.*, 1979], 205°C for zircon [*Zeitler et al.*, 1982], and 120°C for apatite [*Dokka et al.*, 1986].

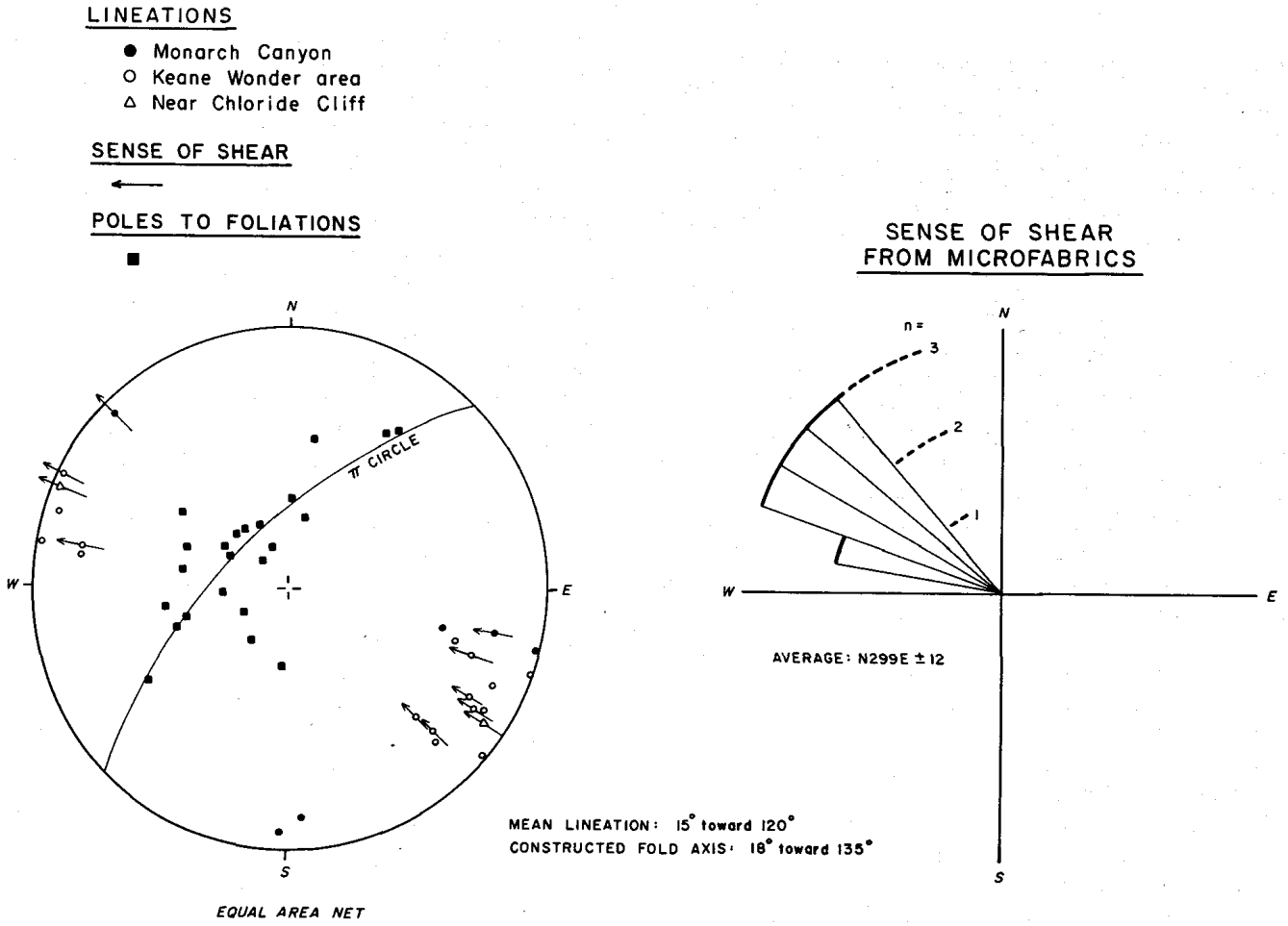

Fig. 13. Lower hemisphere equal area plot of shear sense and orientation data from samples preserving low-temperature ductile microfabrics.

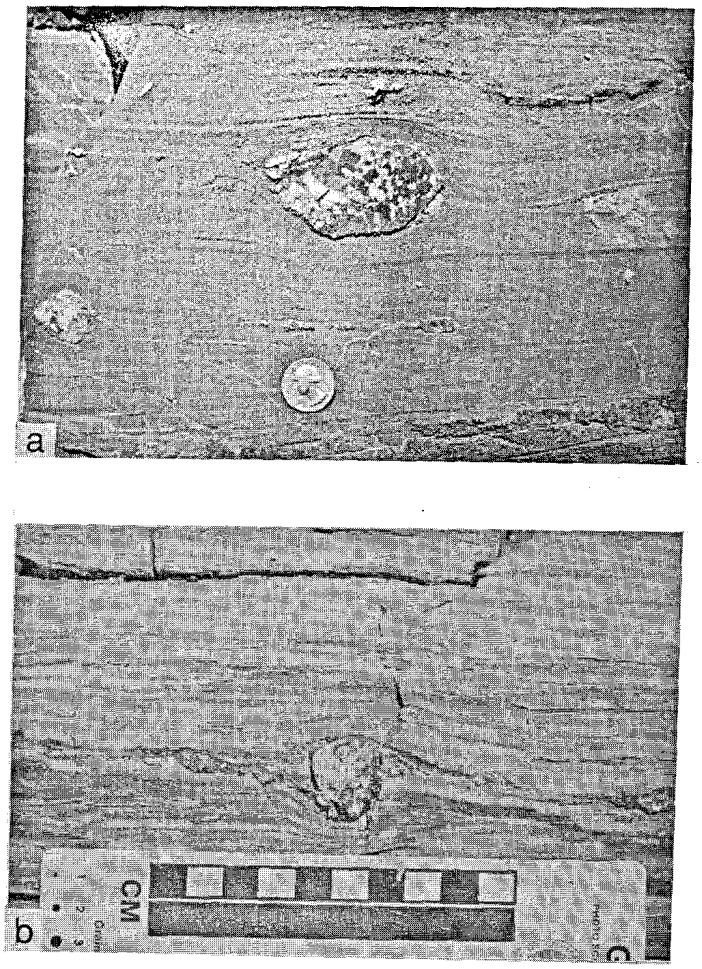

Fig. 14. Mesoscopic shear-sense indicators. (*a*) Location CC-53 (Figure 1, near the Boundary Canyon fault), δ (left of coin) and σ (above coin) quartz porphyroclasts in calc-mylonite indicate sinistral (top-to-the-northwest, toward 293°) movement paralleling the stretching lineation which plunges 3° toward 293°. (*b*) From location CC-74, δ-quartz porphyroclast in calc-mylonite indicates sinistral (top-to-the-northwest, toward 302°) movement paralleling the stretching lineation which plunges 9° toward 122°.

PRESSURE-TEMPERATURE-TIME (P-T-t) PATHS

The P-T-t paths interpreted from the thermobarometric and thermochronologic data (maximum age constraints discussed previously) are shown in Figure 18. At Monarch Canyon, the P-T-t path extends from the peak of metamorphism, 700°C and 9.1 kbar (from geothermobarometry in sample CC-36) in Early Cretaceous time [*DeWitt et al.*, 1988] through ≈500°C (Ar closure temperature in hornblende) sometime after 67 Ma, through ≈350°C (muscovite and biotite Ar-closure temperatures) sometime after 21 Ma, and through the interval 285°–120°C (fission track closure temperatures in titanite and apatite) within 11–6 Ma. Exposure to the surface occurred sometime after 6 Ma. The P-T-t path must pass through the sillimanite stability field to account for the presence of sillimanite.

The combined Chloride Cliff and Keane Wonder areas cooled from the inferred peak of metamorphism, 590°C and 7.3 kbar (average from Figure 5) in Early Cretaceous time, through ≈500°C (Ar closure temperature in hornblende) sometime after 113 Ma, through ≈350°C (Ar closure temperature in muscovite) sometime after 51 Ma, and through 120°C (fission track closure temperature in apatite) at 6 Ma. Exposure to the surface occurred sometime after 6 Ma. No sillimanite has ever been observed or reported outside Monarch Canyon, which suggests that the P-T-t path at Chloride Cliff does not pass through the sillimanite stability field.

Further constraints on the P-T-t paths are obtained from the isograds (Figure 1). Metamorphic mineral assemblages, which form the basis for the isograds, are likely to be inherited along the highest-temperature portion of a P-T-t path [*Thompson and England*, 1984]. The highest-temperature portions of the paths in the Monarch Canyon and Chloride Cliff-Keane Wonder areas should therefore reside at temperatures above the discontinuous AFM reactions which limit the staurolite and kyanite zones, respectively (R1 and R2 in Figure 18).

The P-T-t paths in Figure 18 are one interpretation of the thermochronologic and thermobarometric data, but problems with excess ^{40}Ar in the K-Ar and $^{40}Ar/^{39}Ar$ data sets make other interpretations possible. One aspect of the interpretation is that cooling ages in the Monarch Canyon area are younger than in the Chloride Cliff-Keane Wonder area. It is possible, however, that cooling through Ar-closure temperatures took place at the same time in both the Monarch Canyon and Chloride Cliff-Keane Wonder areas, or that the age relationship is reversed, with cooling in Monarch Canyon taking place before the Chloride Cliff-Keane Wonder area. Both of these alternatives require that cooling ages in the Chloride Cliff-Keane Wonder area be much younger than the maximum age constraints determined in this study. Additionally, the peak of metamorphism may be younger than the Early Cretaceous age inferred by *DeWitt et al.* [1988] from $^{40}Ar/^{39}Ar$ data. Only with additional data will the cooling history be firmly established. Nevertheless, it may not be a coincidence that the maximum age constraints derived from all three minerals dated (muscovite, biotite, and hornblende) are significantly younger (27–46 m.y.) in the Monarch Canyon area than in the Chloride Cliff-Keane Wonder area.

Because of uncertainties, the thermobarometric data do not independently prove that there was a difference in pressure associated with the peak of metamorphism between Monarch Canyon (9.1 kbar) and the Chloride Cliff-Keane Wonder area (5.5–7.7 kbar). The evidence documenting a difference in temperature (700°C in Monarch Canyon, 590°C at Chloride Cliff) is more compelling, with confirmation provided by garnet-biotite geothermometry, the R2 isograd, the presence (Monarch Canyon) versus absence (Chloride Cliff) of sillimanite, and homogenized garnets (Monarch Canyon, CC-33a in Figure 4, and Figure 5 from *Hodges and Walker* [1990]) versus growth-zoned garnets (Chloride Cliff, CC-72d in Figure 4). There are two possible ways in which the difference in temperature might be explained, it could be due to a difference in depth or to heat introduced in Monarch Canyon by the Late Cretaceous muscovite granite dikes. If the dikes were anatectic in origin and locally derived, as speculated by *Applegate et al.* [1992], then the timing of peak temperatures must conform to the Late Cretaceous age of the dikes, which is in disagreement with the Early Cretaceous age of peak metamorphism inferred by *DeWitt et al.* [1988] from $^{40}Ar/^{39}Ar$ data. In such a case, the dikes could not have caused heating in Monarch Canyon but would have been products of the high-temperature metamorphism. If the melts were derived from deeper levels, then

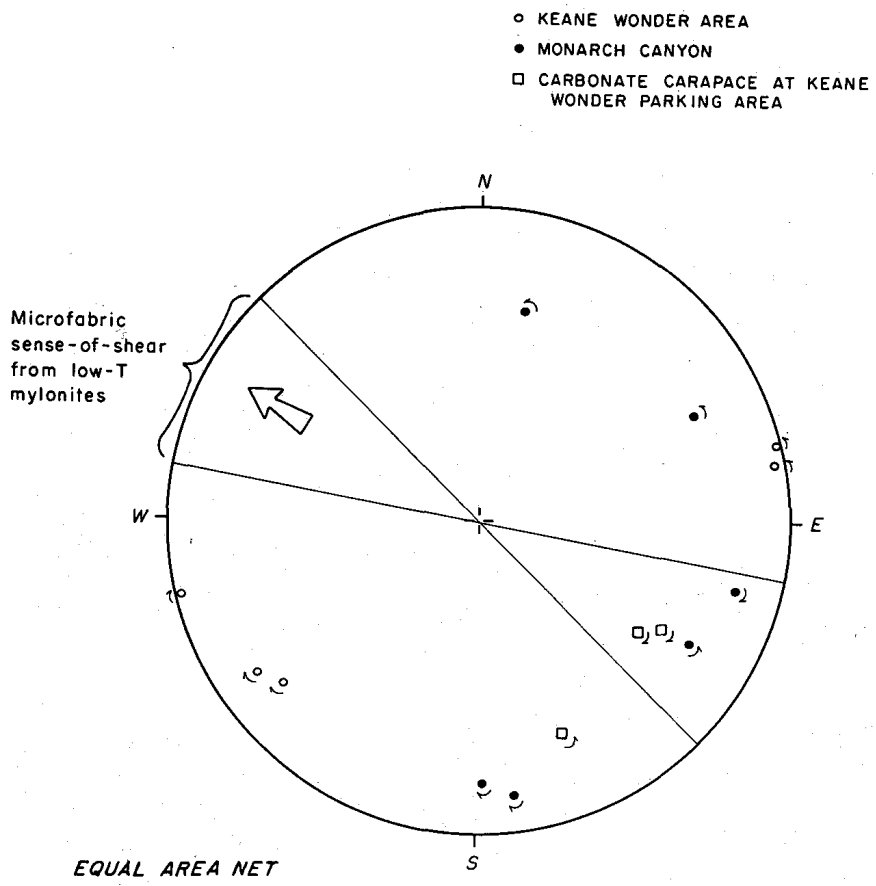

Fig. 15. Lower hemisphere equal area plot of fold axes and overturning directions showing inferred movement direction (method of *Hansen* [1971]). Microfabric shear sense is from Figure 13.

they could have injected upward and caused heating, but such heating would have been confined largely to the margins of the dikes [*Jaeger*, 1957]. This is consistent with the findings of *DeWitt et al.* [1988], who concluded that hornblende from a sample of country rock had been reset in Late Cretaceous time by heat from an adjacent dike. The small-volume proportion of dikes (20%) and the fact that they intruded over several million years [*Applegate et al.*, 1992], which would have allowed heat to dissipate quickly relative to the rate of introduction, argue against the dikes having had a large regional thermal impact. The distribution of dikes, 20% at Monarch Canyon decreasing to almost none at Chloride Cliff, may be an artifact of differing vertical proximity to the source of melts.

A Possible Interpretation

If the P-T-t paths in Figure 18 are correct, then there are important implications for the uplift and tectonic history. One approach to interpreting the thermobarometric data was to regard the peak of metamorphism as associated with a geothermal gradient (probably not steady state) of 22°C km^{-1}. Accordingly, geothermometry from Monarch Canyon (700°C), Chloride Cliff (590°C), Indian Pass (490°C), and the southern Funeral Mountains (≈350°C) indicate depths of 32, 27, 22, and 16 km, respectively. This satisfies the thermobarometry from Monarch Canyon (9.1 kbar or 32 km depth) and Chloride Cliff (5.5–7.7 kbar or 19–27 km) and is consistent with the presence of kyanite at Indian Pass. Isograd reactions R1 and R2 are also correctly placed by this approach, as depicted in a reconstruction of the area at the time of peak metamorphism (Figure 19). The reconstruction places (R1), the lower-temperature boundary of the staurolite zone, at precisely the conditions indicated in the petrogenetic grid of *Spear and Cheney* [1989], and places R2, the lower boundary of the kyanite zone, at conditions 20°C lower (or approximately 1 km shallower) than indicated by *Spear and Cheney* [1989]. Stratal thicknesses [*Hunt and Mabey*, 1966; *Stewart*, 1970] are about half that needed to account for the observed variation in pressure and temperature with a gradient of 22°/km. A moderate northwest dip of the sedimentary package reconciles the stratal thicknesses with the variation in pressure and temperature (Figure 19). This is consistent with the reconstruction of *Wernicke et al.* [1988], who also placed units in the lower plate in a northwest dipping orientation prior to Neogene extension. Schematic thrust faults are drawn in the reconstruction (Figure 19) to convey a thrust loading concept [e.g., *Wernicke et al.*, 1988], although details of the overlying thrust geometries are unknown.

The P-T-t paths (Figure 18) are consistent with the Chloride Cliff-Keane Wonder area being at shallower crustal levels than the Monarch Canyon area throughout most of the uplift history, the Chloride Cliff-Keane Wonder area cooling through Ar-closure temperatures in muscovite, biotite and hornblende 27–46 m.y. before the Monarch Canyon area. Cooling related to uplift was ongoing by late Early Cretaceous time, as indicated by passage through the Ar-closure temperature in hornblende (≈500°C) at Chloride Cliff at 113 Ma (Figure 17). In Late Cretaceous time, muscovite granite dikes injected upward into the cooling package of rocks,

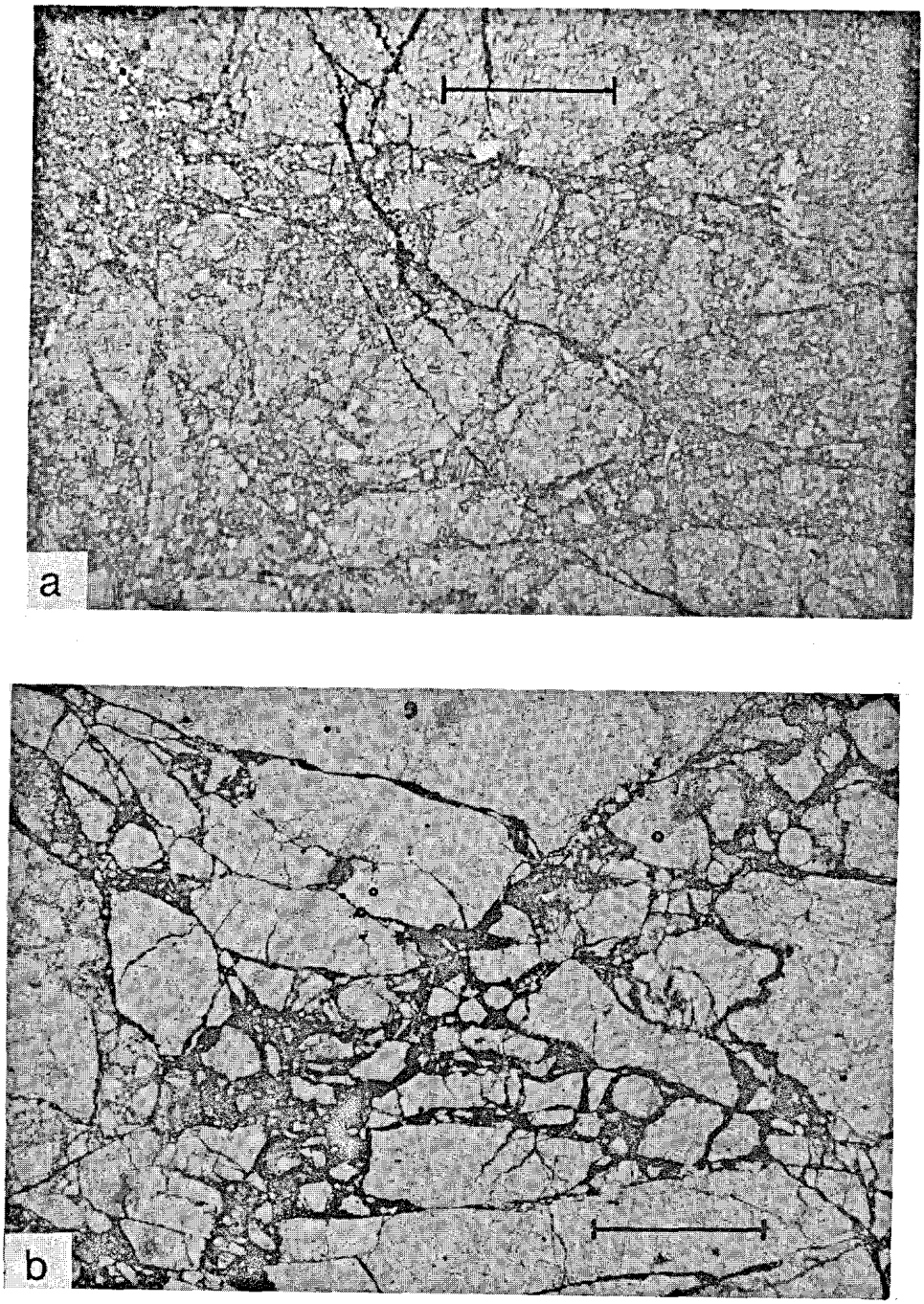

Fig. 16. Photomicrographs of samples from the upper and lower plates at the contact with the Boundary Canyon fault (location CC-54, Figure 1). Scale bars are 1 mm long. (*a*) Cracked dolomite marble from lower plate (CC-54b). Plane-polarized light. (*b*) Cracked quartz from Stirling Quartzite (CC-54c) of the upper plate. Plane-polarized light.

having been generated by melting at depth possibly as a result of decompression [cf. *Applegate et al.*, 1992]. Apatite fission track data (Table 4 and *Holm and Dokka* [1991] indicate that both the Monarch Canyon and Chloride Cliff-Keane Wonder areas were at approximately the same crustal level by 6 Ma, which was accomplished by a strong (60°–80°) tilt to the southeast. Cooling through Ar-closure temperatures in muscovite and biotite at 21 Ma in Monarch Canyon (Table 3) confines the tilting to have taken place within the interval 21–6 Ma. Generally, westward movement of the upper plate within the interval 9–5 Ma inferred by *Reynolds et al.* [1986] and rapid cooling in the Monarch Canyon area within the interval 11–6 Ma inferred from fission track data indicate that tilting and rapid uplift were closely associated in timing with movement along the detachment fault. Apatite fission track data indicate that exposure of the lower plate to the surface occurred sometime after 6 Ma. This interpretation is broadly consistent with current theories of detachment fault evolution [*Buck*, 1988; *Hamilton*, 1988*a*, *b*; *Wernicke and Axen*, 1988; *Spencer and Reynolds*, 1991] in which the fault surface rotates from an initially dipping orientation to subhorizontal, while the lower plate undergoes a comparable tilt.

There is a continuum of ductile fabrics inherited at different points during cooling, with top-to-the-northwest movement inferred for all of them. U-Pb dating of deformed and undeformed Late Cretaceous muscovite granites indicate that ductile deformation in Precambrian gneiss was ongoing

TABLE 3. Conventional K-Ar Dating of Minerals From the Northern Funeral Mountains

Sample	Mineral	Weight % K_2O	$^{40}Ar_{rad}$, moles/g	$^{40}Ar_{rad}/^{40}Ar_{total}$	Calculated Age, Ma	Location[a]	
						Latitude/Longitude	Locality
82-38[b]	Biotite	8.77	2.704×10^{-10}	0.53	21.3 ± 0.5		Monarch Canyon
(1.7 Ga biotite granite)	Muscovite	10.89	3.305×10^{-10}	0.44	21.0 ± 0.5	36°43'N/116°55'W	
82-39[b]	Biotite	8.135	6.031×10^{-10}	0.66	50.8 ± 1.3		Monarch Canyon
(biotite hornblende schist)	Hornblende	0.762	7.536×10^{-10}	0.42	67.4 ± 1.7		
CC-58[c]	Biotite	7.91	8.592×10^{-10}	0.87	73.9 ± 1.8	36°43.0'N/116°55.7'W	Monarch Canyon
(pelitic schist)	Muscovite	8.875	5.660×10^{-10}	0.75	43.8 ± 1.1		
JN85CC-3[c] Canyon (amphibolite)	Hornblende	0.286	2.610×10^{-10}	0.86	543.2 ± 13.6	36°44.0'N/116°54.75'W	Monarch Canyon
JN85CC-4[c] (muscovite schist)	Muscovite	8.22	7.552×10^{-10}	0.90	62.7 ± 2.3		Monarch Canyon
JN85CC-1[c] (muscovite schist)	Muscovite	8.89	6.603×10^{-10}	0.35	50.9 ± 1.3		Keane Wonder Mine visitor parking area
JN85CC-2[c]	Biotite	7.57	5.335×10^{-10}	0.65	48.3 ± 1.2	36°40.0'N/116°54.5'W	Keane Wonder
(biotite hornblende schist)	Hornblende	0.813	1.622×10^{-10}	0.79	133.6 ± 3.3		Mine visitor parking area

[a]Sample locations are plotted in Figure 1.
[b]Source: J. C. VonEssen (written communication to M. D. Carr, 1983).
[c]Source: J. K. Nakata (writen communication to T. D. Hoisch, 1991).

at 72 Ma in Monarch Canyon [*Applegate et al.*, 1992]. Quartz mylonites from Monarch Canyon formed at temperatures below 480°C and above 325°C (from previous discussion of grain size and textural characteristics), sometime between 67 Ma (K-Ar age in hornblende, Table 3) and 11 Ma (fission track age in zircon [*Holm and Dokka*, 1991]). The transition from ductile to brittle behavior in quartz in the Monarch Canyon area should have taken place between 21–6 Ma, during which time the area cooled through the interval 350°–120°C (closure temperatures for Ar in muscovite and apatite fission tracks). The pervasively deformed rocks of the lower plate may represent a wide northwest dipping shear zone which accommodated the early phase of uplift before the development of a discrete fault and southeast tilting. Normal-sense movement along the shear zone is consistent with the rise of formerly very deep rocks to the surface and with kinematic indicators. The width of the shear zone is unknown because the top is truncated by the detachment fault and the bottom is presently unseen, but must be at least as wide as the present structural depth beneath the detachment fault in the northern Funeral Mountains (≈700 m). The parallelism of ductile fabrics with the present detachment fault surface suggests that the fault developed when lower plate rocks rose and cooled through the transition from ductile to brittle regimes. The calc-mylonites from the Keane Wonder Mine visitor parking area and near the Boundary Canyon fault formed at temperatures below that of the quartz mylonites and indicate the same northwest vergence; field evidence suggests that they formed during fault movement [*Hamilton*, 1988*a*], by which time quartz was behaving brittley. Folds within the lower plate and in the calc-mylonites along the fault surface formed during uplift and cooling as a consequence of the same northwest directed shear.

The data in this study do not independently constrain the shape or dip of the fault surface at the time of nucleation, which would be important for distinguishing among the various models of fault evolution. However, if the present interpretation is correct, then between Monarch Canyon and Chloride Cliff, the fault nucleated with a moderate northwest dip, slightly greater than bedding, cutting across strata at low angle. A subsequent rotation of the fault surface to a subhorizontal orientation, contemporaneous with the migration of a flexural hinge to the northwest, would have resulted in the southeast tilt of the lower plate. This is broadly consistent with the interpretation of *Hamilton* [1988*a*, *b*], whose regional synthesis concluded that the flexural hinge migrated westward.

Tectonic reconstruction along the movement vector

TABLE 4. Fission Track Analysis of Apatite From Pelitic Schist Sample CC-61

	Value
Number of Grains	8
Spontaneous Track Density, tracks cm^{-3} (tracks counted)	7.76×10^4 (69)
Induced Track Density, tracks cm (tracks counted)	6.33×10^6 (2812)
Chi-Square Probability	P
Standard Track Density, tracks cm^{-2} (tracks counted)	4.30×10^4 (5075)
Age, Ma $\pm 2\sigma$	5.6 ± 1.4

Zeta (SRM 963) = 10672; P is pass chi-square test at 5% (external detector runs). Laboratory sample number is DF-6108. Analyzed by C. W. Naeser (written communication to M. D. Carr, 1990). The very low fossil track density prevented determination of the track length in this sample. Sample is from Chloride Cliff (location in Figure 1).

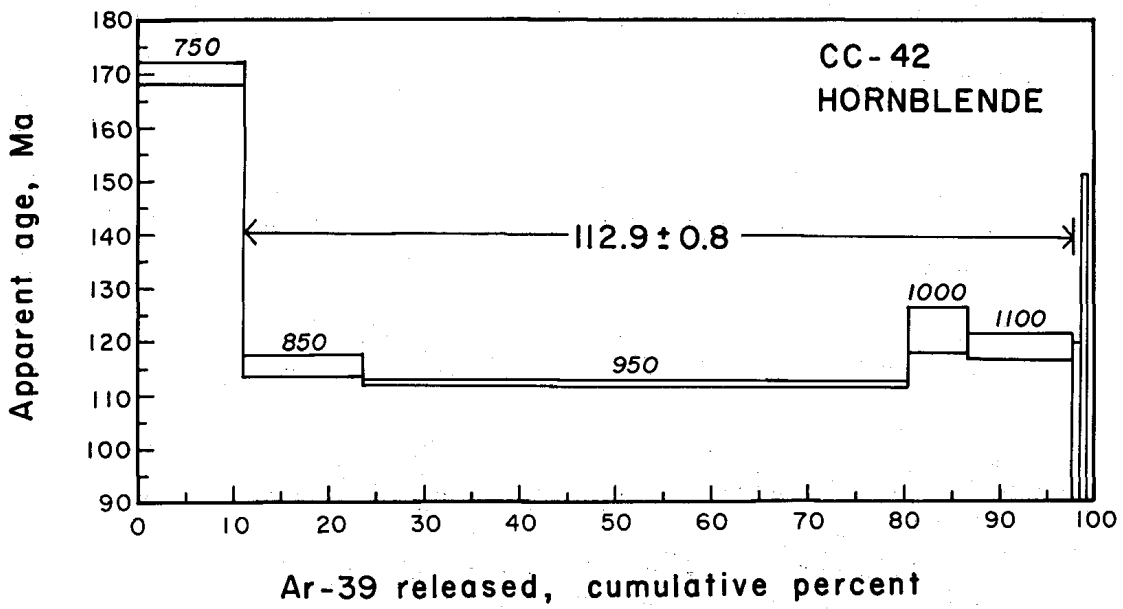

Fig. 17. $^{40}Ar/^{39}Ar$ age spectrum for hornblende from sample CC-42, an undeformed garnet amphibolite (metamorphosed basaltic dike) from Chloride Cliff (location in Figure 1). Numbers in italics denote the temperatures (in degrees Celsius) at which gas increments were evolved. Weighted age of the plateau (increments 850°–1100°C) is 112.9 ± 0.8 (1σ) Ma.

places the Grapevine Mountains over the Funeral Mountains, joining the low-grade Lower Cambrian units mapped by *Reynolds* [1969] in the southern Grapevine Mountains to the same low-grade Lower Cambrian units mapped by *McAllister* [1971] in the southern Funeral Mountains. This represents a minimum displacement of 40 km. Features such as the Titus Canyon anticline in the Grapevine Mountains and the Winters Peak anticline in the southern Funeral Mountains may have been initially joined [*Snow and Wernicke*, 1990]. To bring these two features into alignment

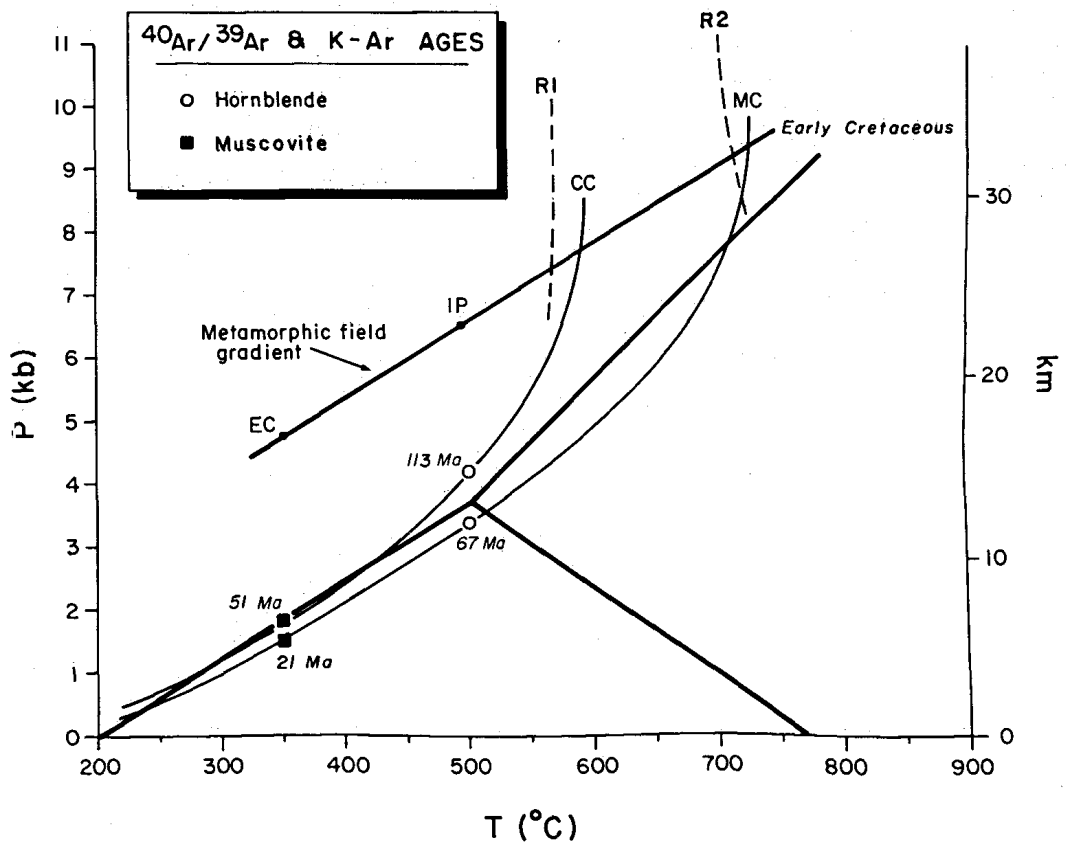

Fig. 18. P-T-t paths for the northern Funeral Mountains. Al_2SiO_5 stability fields of *Holdaway* [1971] are shown. R1 and R2 are the isograd reactions [from *Spear and Cheney*, 1989]. Maximum cooling age constraints for muscovite and hornblende are indicated (see text for detailed discussion of $^{40}Ar/^{39}Ar$ and K-Ar data). CC is Chloride Cliff, EC is Echo Canyon, IP is Indian Pass, and MC is Monarch Canyon.

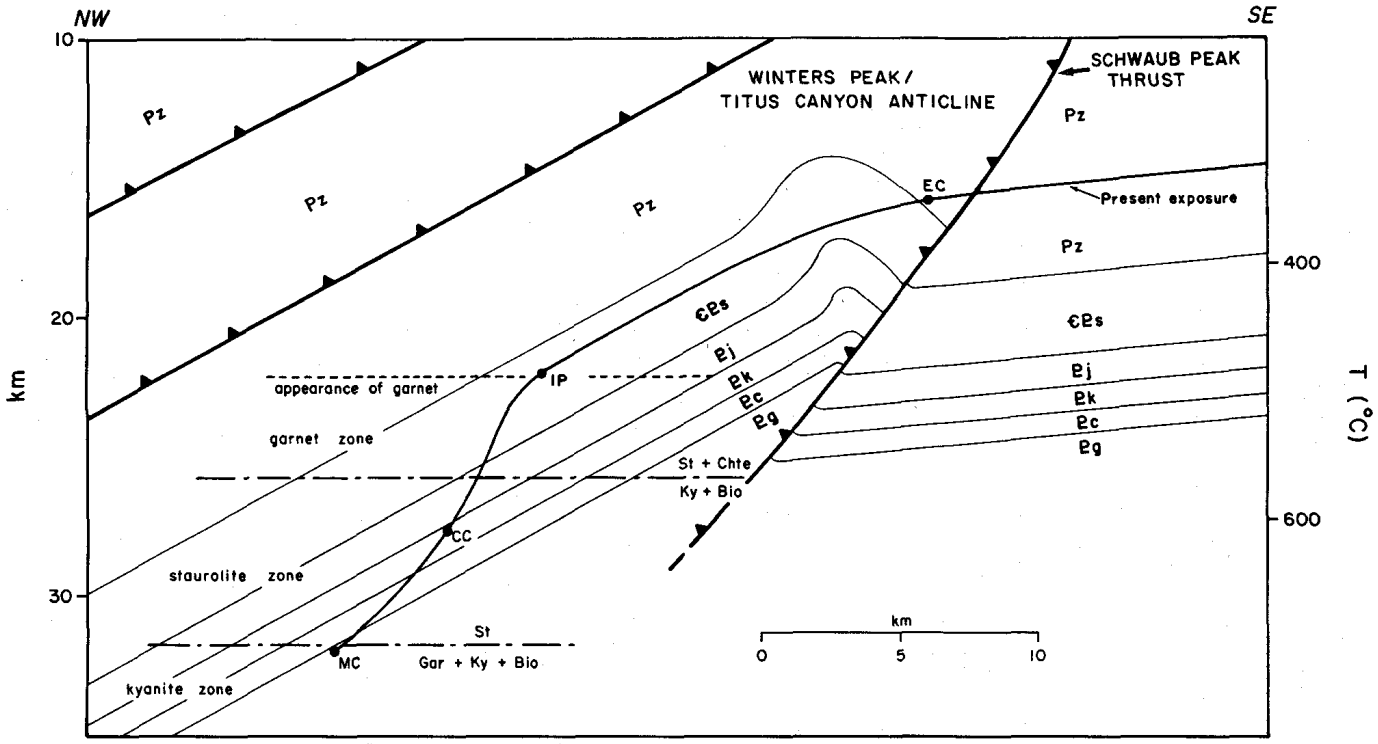

Fig. 19. Schematic cross section for Early Cretaceous (?) time, at peak of metamorphism, showing orientation of the Funeral Mountains, isograds, metamorphic zones, and positions of major structural features. See Table 1 for mineral abbreviations. MC is Monarch Canyon (location CC-36); CC is Chloride Cliff (location CC-25/61/72); IP is Indian Pass (location CC-68); and EC is Echo Canyon. Distances between labeled locations have been adjusted to remove offsets along Tertiary normal faults (based upon G-G″ cross section of *Wright et al.* [1989]). Schematic overlying thrust faults are drawn to convey a thrust loading concept [*Wernicke et al.*, 1988], but actual geometries are unknown. Unit symbols are the same as Figure 1, except that "Pz" is the Paleozoic section beginning with the Cambrian Wood Canyon Formation and extending at least to the top of the Upper Mississippian Rest Spring Shale.

would require that the Grapevine Mountains be rotated 90° counterclockwise along a vertical axis from its predisplacement orientation. *Snow and Wernicke* [1990] believe that pieces of the same anticline are also present in several other nearby mountain ranges and used them to support an analysis of Neogene displacements.

Acknowledgments. Field excursions with M. D. Carr, W. B. Hamilton, B. W. Troxel, and L. A. Wright contributed greatly to establishing a framework for carrying out this study. Numerous discussions with them and with E. DeWitt proved essential and enlightening; however, the views expressed in this paper are not necessarily shared by these individuals. We thank DeWitt for providing a copy of his unpublished $^{40}Ar/^{39}Ar$ data, J. K. Nakata for his K-Ar and $^{40}Ar/^{39}Ar$ dating of minerals, and C. W. Naeser for his fission track analysis of apatite in sample CC-61. Comments by Carr, Hamilton, R. LeCompte, M. L. Wells, and an anonymous reviewer were very helpful. We thank K. F. Fox, Jr., for providing the sample and location for KF18 and H. R. Wenk for consultations concerning microfabrics preserved in calc-mylonites. We thank Carr for his assistance in coordinating the K-Ar, $^{40}Ar/^{39}Ar$ and fission track analytical work and making available several important written communications. This project was initiated as part of a National Research Council-U.S. Geological Survey Research Associateship to TDH. Additional work was supported by the U.S. Geological Survey in cooperation with the U.S. Department of Energy under interagency agreement DE-AI08-78ET44802.

REFERENCES

Applegate, J. D. R., J. D. Walker, and K. V. Hodges, Late Cretaceous extensional unroofing in the Funeral Mountains metamorphic core complex, California, *Geology*, *20*, 519–522, 1992.

Berthé, D., P. Choukroune, and P. Jegouzo, Orthogneiss, mylonite and non-coaxial deformation of granites: The example of the South Armorican shear zone, *J. Struct. Geol.*, *1*, 31–42, 1979.

Buck, W. R., Flexural rotation of normal faults, *Tectonics*, *7*, 959–973, 1988.

Corbett, K., C. T. Wrucke, and C. A. Nelsen, Structure and tectonic history of the Last Chance Thrust system, Inyo Mountains and Last Chance Range, California, in This Extended Land, Geological Journeys in the Southern Basin and Range, Geological Society of America, Cordilleran Section, Field Trip Guidebook, edited by D. L. Weide and M. L. Faber, *Spec. Publ. 2*, pp. 269–292, Univ. of Nev. Geosci. Dep., Las Vegas, 1988.

DeWitt, E., J. F. Sutter, L. A. Wright, and B. W. Troxel, Ar-Ar chronology of Early Cretaceous regional metamorphism, Funeral Mountains, California—A case study of excess argon, *Geol. Soc. Am. Abstr. Programs*, *20*, A16, 1988.

Dokka, R. K., M. J. Mahaffie, and A. W. Snoke, Thermochronologic evidence of major tectonic denudation associated with detachment faulting, northern Ruby Mountains–East Humbolt Range, Nevada, *Tectonics*, *5*, 995–1006, 1986.

Edward, G. H., M. A. Etheridge, and B. E. Hobbs, On the stress dependence of subgrain size, *Textures Microstruct.*, *5*, 127–152, 1982.

England, P. E., and A. B. Thompson, Pressure-temperature-time paths of regional metamorphism, I, Heat transfer during the evolution of regions of thickened continental crust. *J. Petrol.*, *25*, 894–928, 1984.

Frost, B. R., and T. Chacko, The granulite uncertainty principle: Limitations on thermobarometry in granulites, *J. Geol.*, *97*, 435–450, 1989.

Giaramita, M. J., Structural evolution and metamorphic petrology of the Monarch Canyon area, northern Funeral Mountains, Death Valley, California, M.S. thesis, 145 pp., Univ. of Calif., Davis, 1984.

Grambling, J. A., Internally-consistent geothermometry and H_2O barometry in metamorphic rocks: The example garnet-chlorite-quartz, *Contrib. Mineral. Petrol.*, *105*, 617–628, 1990.

Hamilton, W. B., Detachment faulting in the Death Valley region, California and Nevada, *U.S. Geol. Surv. Bull. 1790*, 51–85, 1988*a*.

Hamilton, W. B., Death Valley tectonics—Hingeline between active and inactivated parts of a rising and flattening master normal fault, in *Geology of the Death Valley Region*, edited by J. L. Gregory and E. J. Baldwin, *Field Trip Guideb.*, vol. 16, pp. 179–205, South Coast Geological Society, Santa Ana, Calif., 1988*b*.

Hansen, E., *Strain Facies*, 207 pp., Springer-Verlag, New York, 1971.

Harris, A. G., B. R. Wardlaw, C. C. Rust, and G. K. Merrill, Maps for assessing thermal maturity (conodont color alteration index maps) in Ordovician through Triassic rocks in Nevada and Utah and adjacent parts of Idaho and California, *U.S. Geol. Surv. Misc. Invest. Ser. Map, I-1249*, 1980.

Harrison, T. M., R. L. Armstrong, C. W. Naeser, and J. E. Harakal, Geochronology and thermal history of the Coast Plutonic Complex, near Prince Rupert, British Columbia, *Can. J. Earth Sci.*, *16*, 400–410, 1979.

Hodges, K. V., and F. S. Spear, Geothermometry, geobarometry and the Al_2SiO_5 triple point at Mt. Moosilauke, New Hampshire, *Am. Mineral.*, *67*, 1118–1134, 1982.

Hodges, K. V., and J. D. Walker, Petrologic constraints on the unroofing history of the Funeral Mountains metamorphic core complex, California, *J. Geophys. Res.*, *95*, 8437–8445, 1990.

Hoisch, T. D., A muscovite-biotite geothermometer, *Am. Mineral.*, *74*, 565–572, 1989.

Hoisch, T. D., Empirical calibration of six geobarometers for the mineral assemblage quartz + muscovite + biotite + plagioclase + garnet, *Contrib. Mineral. Petrol.*, *74*, 225–234, 1990.

Hoisch, T. D., Equilibria within the mineral assemblage quartz + muscovite + biotite + garnet + plagioclase, and implications for the mixing properties of octahedrally-coordinated cations in muscovite and biotite, *Contrib. Mineral. Petrol.*, *108*, 43–54, 1991.

Holdaway, M. J., Stability of andalusite and the aluminum silicate phase diagram, *Am. J. Sci.*, *271*, 97–131, 1971.

Holm, D. K., and R. K. Dokka, Major late Miocene cooling of the middle crust associated with extensional orogenesis in the Funeral Mountains, California, *Geophys. Res. Lett.*, *18*, 1775–1778, 1991.

Hunt, C. B., and D. R. Mabey, Stratigraphy and structure, Death Valley, California, *U.S. Geol. Surv. Prof. Pap.*, *494-A*, 162 pp., 1966.

Jaeger, J. C., The temperature in the neighborhood of a cooling intrusive sheet, *Am. J. Sci.*, *255*, 306–318, 1957.

Kohn, M. J., and F. S. Spear, Error propagation for barometers, 2, Application to rocks, *Am. Mineral.*, *76*, 138–147, 1991.

Koziol, A. M., and R. C. Newton, Redetermination of the anorthite breakdown reaction and improvement of the plagioclase-garnet-Al_2SiO_5 geobarometer, *Am. Mineral.*, *73*, 216–223, 1988.

Labotka, T. C., Petrology of a medium-pressure regional metamorphic terrane, Funeral Mountains, California, *Am. Mineral.*, *65*, 670–689, 1980.

Labotka, T. C., and A. Albee, Metamorphism and tectonics of the Death Valley region, California and Nevada, in *Metamorphism and Crustal Evolution of the Western United States*, edited by W. G. Ernst, pp. 715–736, Prentice-Hall, Englewood Cliffs, N. J., 1988.

Lister, G. S., and A. W. Snoke, S-C mylonites, *J. Struct. Geol.*, *6*, 617–638, 1984.

McAllister, J. F., Preliminary map of the Funeral Mountains in the Ryan Quadrangle, Death Valley Region, Inyo County, California, scale 1:31,680, *U.S. Geol. Surv. Open File Rep.*, *71-187*, 1971.

McDougall, I., and T. M. Harrison, *Geochronology and Thermochronology by the $^{40}Ar/^{39}Ar$ Method*, 212 pp., Oxford University Press, New York, 1988.

Passchier, C. W., and C. Simpson, Porphyroclast systems as kinematic indicators, *J. Struct. Geol.*, *8*, 831–843, 1986.

Pierce, M. L., and J. M. Christie, Dislocation recovery in quartz aggregates during annealing (abstract), *Eos Trans. AGU*, *68*, 422, 1987.

Poirier, J. P., and A. Nicholas, Deformation-induced recrystallization by progressive misorientation of subgrain boundaries, with special reference to mantle peridotite, *J. Geol.*, *83*, 707–720, 1975.

Rejebian, V. A., A. G. Harris, and J. S. Heubner, Conodont color and textural alteration: An index to regional metamorphism, contact metamorphism, and hydrothermal alteration, *Geol. Soc. Am. Bull.*, *99*, 471–479, 1987.

Reynolds, M. W., Stratigraphy and structural geology of the Titus and Titanothere Canyons areas, Death Valley, California, Ph.D. thesis, 406 pp., Univ. of Calif., Berkeley, 1969.

Reynolds, M. W., Geology of the Grapevine Mountains, Death Valley, California: A summary, in Geologic Features, Death Valley, California, edited by B. W. Troxel and L. A. Wright, *Spec. Rep. Calif. Div. Mines Geol.*, *106*, 19–25, 1976.

Reynolds, M. W., L. A. Wright, and B. W. Troxel, Geometry and chronology of late Cenozoic detachment faulting, Funeral and Grapevine Mountains, Death Valley, California, *Geol. Soc. Am. Abstr. Programs*, *18*, 175, 1986.

Schmid, S. M., R. Panozzo, and S. Bauer, Simple shear experiments on calcite rocks: Rheology and microfabric, *J. Struct. Geol.*, *9*, 747–778, 1987.

Simpson, C., and S. M. Schmid, An evaluation of criteria to deduce the sense of movement in sheared rocks, *Geol. Soc. Am. Bull.*, *94*, 1281–1288, 1983.

Snow, J. K., and B. Wernicke, Uniqueness of geological correlations: An example from the Death Valley extended terrain, *Geol. Soc. Am. Bull.*, *101*, 1351–1362, 1990.

Snow, J. K., Y. Asmerom, and D. R. Lux, Permian-Triassic plutonism and tectonics, Death Valley region, California and Nevada, *Geology*, *19*, 629–632, 1991.

Spear, F. S., Petrologic determination of metamorphic pressure-temperature-time paths, in *Metamorphic Pressure-Temperature-Time Paths, Short Course Geol.*, vol. 7, edited by M. F. Crawford and E. Padovani, pp. 1–55, AGU, Washington, D. C., 1989.

Spear, F. S., and J. T. Cheney, A petrogenetic grid for pelitic schists, *Contrib. Mineral. Petrol.*, *101*, 149–164, 1989.

Spear, F. S., and F. P. Florence, Thermobarometry in granulites: Pitfalls and new approaches, *Precambrian Res.*, *55*, 209–241, 1992.

Spear, F. S., and J. Selverstone, Quantitative P-T paths from zoned minerals: Theory and tectonic applications, *Contrib. Mineral. Petrol.*, *83*, 348–357, 1983.

Spencer, J. E., and S. J. Reynolds, Tectonics of mid-Tertiary extension along a transect through west central Arizona, *Tectonics*, *10*, 1204–1221, 1991.

Stewart, J. H., Upper Precambrian and Lower Cambrian strata in the southern Great Basin California and Nevada, *U.S. Geol. Surv. Prof. Pap.*, *620*, 206 pp., 1970.

Thompson, A. B., and P. C. England, Pressure-temperature-time paths of regional metamorphism, II, Their inference and interpretation using mineral assemblages and metamorphic rocks, *J. Petrol.*, *25*, 929–955, 1984.

Thompson, J. B., The graphical analysis of mineral assemblages in pelitic schists, *Am. Mineral.*, *42*, 842–858, 1957.

Tracy, R. J., Compositional zoning and inclusions in metamorphic minerals, in Characterization of Metamorphism Through Mineral Equilibria, edited by J. M. Ferry, *Rev. Mineral.*, *10*, 355–397, 1982.

Troxel, B. W., and L. A. Wright, Geologic map of the central and northern Funeral Mountains and adjacent areas, Death Valley region, southern California, *U.S. Geol. Surv. Open File Rep.*, *89-348*, 1989.

Tullis, J. A., and R. A. Yund, Hydrolytic weakening of experimentally deformed Westerly granite and Hale albite rock, *J. Struct. Geol.*, *2*, 439–451, 1980.

Tullis, J. A., and R. A. Yund, Grain growth kinetics of quartz and calcite aggregates, *J. Geol.*, *90*, 301–318, 1982.

Twiss, R. J., Theory and applicability of a recrystallized grain size paleopiezometer, *Pure Appl. Geophys.*, *115*, 227–244, 1977.

Urai, J. L., W. D. Means, and G. S. Lister, Dynamic recrystallization of minerals, in *Mineral and Rock Deformation: Laboratory Studies—The Paterson Volume, Geophys. Monogr. Ser.*, vol. 36, edited by B. E. Hobbs and H. C. Heard, pp. 161–199, AGU, Washington, D. C., 1986.

Wenk, H. R., T. Takeshita, E. Bechler, B. G. Erskine, and S. Matthies, Pure shear and simple shear textures, Comparison of experimental, theoretical and natural data, *J. Struct. Geol.*, *9*, 731–746, 1987.

Wernicke, B., and G. J. Axen, On the role of isostasy in the evolution of normal fault systems, *Geology*, *16*, 848–851, 1988.

Wernicke, B., G. J. Axen, and J. K. Snow, Basin and range

extensional tectonics at the latitude of Las Vegas, Nevada, *Geol. Soc. Am. Bull., 100*, 1738–1757, 1988.

Wright, L. A., and B. W. Troxel, Geologic map of the central and northern parts of the Funeral Mountains and adjacent areas, Death Valley region, southern California, scale 1:48,000, *U.S. Geol. Surv. Misc. Invest. Ser. Map, I-2305*, in press, 1993.

Wright, L. A., B. W. Troxel, and J. L. Zigler, Geologic cross sections to accompany geologic map of the central and northern Funeral Mountains and adjacent areas, Death Valley region, southern California, *U.S. Geol. Surv. Open File Rep., 89-647*, 1989.

Zeitler, P. K., N. M. Johnson, C. W. Naeser, and R. A. K. Tahirkheli, Fission-track evidence for Quaternary uplift of the Nanga Parbat region, Pakistan, *Nature, 298*, 255–257, 1982.

Zeuch, D. H., On the inter-relationship between grain size sensitive creep and dynamic recrystallization of olivine, *Tectonophysics, 93*, 151–168, 1983.

T. D. Hoisch, Department of Geology, Northern Arizona University, Flagstaff, AZ 86011.

C. Simpson, Department of Earth and Planetary Sciences, Johns Hopkins University, Baltimore, MD 21218.

(Received November 15, 1991;
revised September 24, 1992;
accepted October 6, 1992.)